

The MegaCam CFHT CS – StarFEAST and POLU

PIs: Alessandro Boselli, Dustin Lang, and Christophe Yèche

The proposal outlines a MegaCam CFHT Community Survey designed to complement upcoming broad-band surveys such as LSST and Euclid by 2027. It consists of two components using narrow-band and medium-band filters, a unique capability at the CFHT.

The first survey, **StarFEAST**, is aimed at studying the relationship between the star formation process and its surrounding environment (infall, feedback, external perturbations) at different scales, from individual star-forming complexes within the Milky Way, in well resolved Local Group galaxies, in nearby large scale structures, and in the distant ($z \simeq 4.5$) Universe. The selected targets will be observed in a narrow-band $H\alpha$ filter to derive the physical properties of the ionising radiation, tightly related to the star formation activity of the emitting regions with pointed observations over more than 400 deg^2 . Milky Way and local galaxies will also be imaged in the narrow-band [OIII] and [SII] filters to identify the dominant radiation sources responsible for the ionisation of the gas. The data will be used to study the distribution of the ionising radiation, quantify the activity of star formation in different environments and at different scales, from individual HII regions at pc scales, up to cosmological scales. Galaxies in local large scale structures such as the Great Wall and the Perseus Pisces Supercluster will be selected to belong to different density environments, from the rich clusters such as Coma and A1367, to groups of intermediate halo mass, down to filaments and walls. Their comparative analysis will be crucial to quantify the role of the environment on the star formation activity of galaxies. The deep narrow-band images will also be used to detect low surface brightness filaments of gas produced during the interactions of galaxies with their surrounding environment, enabling the identification of the dominant perturbing mechanism in different density regions. They will also be used to identify gas expelled from massive stars in local star-forming complexes, or from the nucleus of massive galaxies, and thus study the feedback process at different scales. The second survey, **POLU**, will cover approximately 4200 deg^2 across both galactic caps and focus on exploring the high-redshift Universe ($z > 2$). By imaging this area with two medium-band filters, covering $4000\text{--}4260\text{\AA}$ and $4260\text{--}4520\text{\AA}$, the survey will enable the selection of Lyman- α Emitters (LAEs) in the redshift range $2.3 < z < 2.7$ and Lyman Break Galaxies (LBGs) in the range $2.5 < z < 3.4$. POLU will be part of a broader coordinated effort involving multiple telescopes, including CFHT, Blanco, and Subaru, together covering around 5000 deg^2 with five medium-band filters in the spectral range 4000\AA to 5300\AA . The scientific motivation is driven by recent results from several cosmological probes suggesting that dark energy (DE) may evolve over cosmic time, a possibility that challenges standard cosmological models. This motivates the need for new high-redshift datasets capable of providing stronger constraints. In this context, the surveys will provide more than three million LAEs and LBGs as targets for the DESI-II spectroscopic program starting in 2029, enabling tests of primordial physics and constraints on DE during the matter-dominated era. Even without spectroscopic follow-up, these samples will allow robust studies of primordial non-Gaussianity through clustering measurements and correlations with CMB lensing. Additionally, POLU will improve photometric redshift calibration for future weak lensing surveys such as Rubin and Euclid, and will also contribute to studies of dark matter in dwarf galaxies.

This survey will require **700 observing nights in dark-grey time, 270 for StarFEAST and 430 for POLU**. Of interest for a wide community since covering science related to the study of the ISM, stellar evolution, galaxy evolution, large-scale structures, high- z galaxies, and cosmology, this survey is based on narrow- and medium-band imaging, taking full advantage of this unique capability of the CFHT. It will provide a reference imaging survey for years to come.

Science justification

1. Narrow and medium band filters as a new vantage point to study the extragalactic Universe

We propose a CFHT Community Survey that will complement ground-based broad-band surveys such as LSST or space-based broad-band surveys such as Euclid for 2027. The project comprises two surveys (see Figure 3 for footprints), one which takes advantage of narrow-band (NB) filters, **StarFEAST**¹, and the other of medium-band (MB) filters, **POLU**². Collectively, these surveys will expand our knowledge of the structure and geometry of the Universe and the baryon cycle leading to the formation of the cosmic structures we see today.

The study of large samples of galaxies detected in wide field, multi-frequency surveys, both in the local Universe and at high redshift, has led to significant progress towards an understanding of the process of galaxy evolution. The sensitivity, angular and spectral resolutions of these surveys have been fundamental in tracing the physical properties of different galaxy components – e.g., stellar populations, multiphase gas, metals, dust, and dark matter – whose content and distribution are tightly connected to the galaxy activity. These achievements have been mirrored by advances in the realism of numerical simulations of galaxy formation. Both observations and simulations consistently point to two main factors as key drivers of galaxy evolution: the secular evolution tightly related to the dynamical mass of the system (Cowie et al. 1996) and the environment in which galaxies reside (Boselli & Gavazzi 2006; Peng et al. 2010). The relative importance of these two factors over cosmic time and mass scales, however, remains elusive. Further progress hinges on the characterisation of astrophysical processes, including gas dynamics, radiative cooling, star formation, and stellar/AGN feedback. Among these, a crucial role is played by star formation, the process which transforms the gas reservoir into new stars, self-regulating cooling and collapse through the injection of thermal or mechanical energy, metals, and dust (Lada 1985). At galactic scales, the process of star formation is modulated by the galaxy environment through gravitational (tidal interactions - Merritt 1983; harassment - Moore et al. 1998) and hydrodynamic interactions (ram pressure stripping (RPS) - Gunn & Gott 1972; thermal evaporation - Cowie & Songaila 1977; starvation - Larson et al. 1980). StarFEAST, with its NB filter sensitivity, will address these questions in a large range of spatial and mass scales, and environments.

At larger, i.e. cosmological, scales, wide galaxy surveys offer a unique opportunity to advance our understanding of DE, inflation and dark matter. Over the past two years, the Dark Energy Spectroscopic Instrument (DESI) has released two sets of cosmological results, revealing evidence for dynamical DE (Adame et al. 2025, Abdul-Karim et al. 2025). This has been recognised as one of the most significant breakthroughs in physics in 2024 and 2025; each of the two articles has already been cited more than 1,000 times. Mapping the $z \gtrsim 2$ Universe will provide significant improvements in the knowledge of DE in the matter-dominated era. In order to explore this uncharted territory, POLU, with two MB filters will allow the selection of novel matter tracers, namely Lyman Break Galaxies (LBG) and galaxies with strong Lyman- α emission known as Ly- α Emitters (LAE). Those LAEs and LBGs could be followed up with DESI, as part of the DESI-II program, to measure their redshift or used directly to study their angular correlation and their cross-correlation with CMB lensing.

MB and NB imaging in survey mode is a unique capability of CFHT/MegaCam, making this facility still competitive in the era of dedicated wide field surveys of the whole sky in broad-bands (e.g. Euclid, LSST). This project is perfectly suited for a Community Survey (CS) since it covers a wide range of topics of major interest for the ISM, stellar evolution, galaxy evolution, large-scale structure, and cosmology, all key areas of interest for the French and Canadian communities. A detailed description of the scientific programs of the two projects follows, along with an analysis of their synergies.

1.1 Scientific Goals of the StarFEAST Survey

StarFEAST is a large, comprehensive, and deep narrow-band (NB) imaging survey of different environments, from star forming complexes within the Milky Way (MW), to local galaxies (LG), in large scale structures including rich clusters, groups of intermediate mass, down to filaments, in the local Universe and at cosmological distances. These data will uncover the physical drivers of the relation between star formation, stellar feedback, and galaxy large scale environment, i.e. how gas density and temperature, metallicity, magnetic fields, kinematics, infall, outflow, stripping affect and are affected by the formation of new stars from Galactic to cosmological scales. We propose deep MegaCam imaging observations in the H α (and partially [SII] and [OIII]) line to reach a point source sensitivity of $F(\text{H}\alpha) = 4 \times 10^{-17} \text{ erg s}^{-1} \text{ cm}^{-2}$ (5σ) and

¹Star Formation in Environments Across Space and Time

²Program of blue Observations on the Large-scale Universe, Polū translates to "blue" in Hawaiian

a surface brightness sensitivity of $\Sigma(H\alpha) = 2 \times 10^{-18} \text{ erg s}^{-1} \text{ cm}^{-2} \text{ arcsec}^{-2}$ (1σ at $3''$ resolution), a sensitivity ~ 2 orders of magnitude deeper than any existing data on this large area ($\sim 400 \text{ deg}^2$) and range of environments, with the exception of the VESTIGE survey at CFHT (100 deg^2 , Boselli et al. 2018a), which however focussed on a single massive cluster.

The acquisition, reduction, and exploitation of the data will be structured in different Working Packages (WP):

WP1.1: Galactic science. (*Leads: A. Zavagno, D. Russeil*)

We plan to observe a wide range of star-forming complexes inside and outside the plane of the MW, spanning a broad range of Galactic longitudes and latitudes, metallicities, dust attenuations and star-formation activities, in order to sample the full range of parameters describing star-formation properties. We will carry out observations in the rest-frame $H\alpha$ filter, the off-band $H\alpha$ filter centred at $\lambda = 6719\text{\AA}$ ([SII] doublet) and the [OIII] filter. The data will be used to trace the distribution of ionised gas using $H\alpha$ emission, an excellent indicator of recent star formation as it is produced by young, massive stars (Kennicutt, 1998). [SII] and [OIII] images will be combined with the $H\alpha$ data in 2D diagnostic diagrams (BPT; Baldwin et al. 1981) to quantify the ionisation state of the gas and find peculiar structures bridging HII regions. When combined with existing data from other wavelengths that sample the physical properties (density, temperature and kinematics) of other gas phases (hot, cold atomic and molecular), dust and free electrons in weak magnetic fields (radio synchrotron and free-free emission; e.g. Fig.1), it will be possible to study the relationship between the cooling processes of the gas, which gives rise to GMCs where star formation occurs, and the impact of stellar feedback on the surrounding medium. This WP is poised to understand the impact of early radiative feedback from massive stars on star formation properties at high angular resolution and sensitivity, finally bridging the gap between Galactic and extragalactic star formation.

WP1.2: Local Galaxies (LG). (*Leads: J. Braine, D. Lokhorst, A.L. Melchior*)

We plan to observe all nearby star-forming galaxies with $\text{Dec} \geq -30^\circ$ listed within the WISE catalogue of Jarrett et al. (2019) with an angular diameter in the W1 band $D_{W1} \geq 7.5 \text{ arcmin}$ (18 objects). These are all nearby objects ($D \lesssim 12 \text{ Mpc}$), including some of the most representative galaxies of the Local Group (M31, M33), spanning a wide range in morphological type (Sab-IBm) and stellar mass ($10^8 \leq M_{star} \leq 10^{11} M_\odot$). The sample also includes a few edge-on systems, where the impact of the feedback in the ejection of gas outside the galactic plane (galactic fountains) can be studied in detail. It also includes a well known nearby group (M81), where the interaction between their members has produced one of the most interesting and spectacular starburst in the nearby Universe (M82). The imaging data will be crucial to identify LSB extended features escaping from the disc and study at unprecedented angular resolution the statistical properties of individual HII regions. Combined with IFU spectroscopic gathered during the MUSE/PHANGS (Emsellem et al. 2022) and SITELLE/SIGNALS (Rousseau-Nepton et al. 2019) surveys of further galaxies, this will be the ideal sample to study at scales $\leq 50 \text{ pc}$ the process of star formation and the associated feedback in different systems, making the link between Galactic HII regions and galaxies in a large variety of environments in nearby large scale structures.

WP1.3: Environmentally driven galaxy evolution in local superclusters. (*Leads: A. Boselli, L. Ferrarese*)

To quantify the impact of the surrounding environment on galaxy evolution we need to observe the widest possible range in galaxy density. The $H\alpha$ -off filter (MP9604) is centered at $\lambda = 6719\text{\AA}$ and is sensitive to the ionised gas emission of star-forming galaxies at $4700 < v_{hel} < 9600 \text{ km s}^{-1}$. This redshift range perfectly matches the velocity range of two large scale structures in the local Universe, the Great Wall (GW) in the spring sky and the Perseus-Pisces supercluster (PPS) in the fall sky. These two structures include massive clusters such as Coma and Perseus ($M_h \sim 10^{15} M_\odot$), several intermediate mass ($M_h \sim 10^{13} M_\odot$) groups, and well defined and identified filaments (Geller & Huchra 1989), and are thus the ideal targets for our proposal. We plan to observe $\sim 400 \text{ deg}^2$, and detect $\gtrsim 3500$ star-forming systems. This deep and large set of data will cover an unprecedented range in halo and galaxy stellar mass ($10^7 \leq M_{star} \leq 10^{12} M_\odot$), providing us with a new angle to perform a statistical, yet highly resolved, study of the physics of environmental effects on the star forming process in the local Universe. The $H\alpha$ images will enable to study the process of star formation down to sub-kpc scales, both in isolated and environmentally affected galaxies down to the dwarf regime. We will also perform a complete census of nuclear outflows, to address the interplay between nuclear starbursts and AGN activity. At the required sensitivity we will detect diffuse ionised gas features extending across several tens of kpc (e.g. Boselli et al. 2016, Fig.1) formed after the interaction of galaxies with their surrounding environment. Such processes are thought to play an important, perhaps fundamental, role in the transformation of star forming galaxies into quiescent systems. Identifying the exact nature (ram pressure stripping, harassment, starvation, etc.) of the perturbing mechanisms, as a function of environment (from filaments to groups and massive clusters), is crucial to constrain cosmological models of galaxy evolution. Combined with tuned models of gas stripping and follow-up observations, these data will reveal the fate of this stripped material in a large range of environments and its contribution to the pollution of the IGM. The tails of ionised gas observed in $H\alpha$ trace the trajectory of galaxies recently accreted in high-density regions (Sun et al. 2026). Combined with radial velocities, they will be used

to study the dynamical evolution of the different substructures of the supercluster and the relation between the quenching process and the infall history of galaxies. Finally, we will test with data, the predictions of high-resolution cosmological hydro-simulations predicting the presence of widespread star formation activity in the ICM (Ahvazi et al. 2024).

WP1.4: A large Volume survey of High-redshift emitters (*Leads: B. Epinat, M. Fossati*)

The H α NB filter will allow us to identify Ly α , [OII] and [OIII] emission-line galaxies at $z=4.5, 0.8,$ and $0.3,$ providing a unique sample of star-forming objects over $\sim 400 \text{ deg}^2$. Indeed, the point-source sensitivity of the survey is comparable to the typical Ly α luminosity of $z=4.5$ galaxies (Ouchi et al. 2008). The data will allow us to extend the sampling of the Ly α LF provided by POLU at $2 < z < 3.2$ to a significantly further distance ($z=4.5$) down to $L(\text{Ly}\alpha) \sim 6 \times 10^{42} \text{ erg s}^{-1}$. From Ly α luminosity functions (Sobral et al. 2018, Tornotti et al. 2025), supplemented by an analysis of the VESTIGE survey data, we estimate that $\sim 60,000$ Ly α and $\sim 15,000$ [OII] and [OIII] emitters will be detected. This sample will provide an unprecedented database for characterising the bright end of the high- z emission line galaxy LF, insensitive to cosmic variance, make the first ever estimate of the Ly α correlation function (Kraljic et al. 2022) at this redshift, and study the variation of the star formation activity with galaxy density in high- z groups and clusters (Boselli et al. 2019, Epinat et al. 2024). The data will thus be highly complementary to those obtained in deep targeted imaging and spectroscopic surveys, which are generally limited to $\simeq 1 \text{ deg}^2$ to jointly constrain the bright and the faint end of the LF (Tornotti et al. 2025). High-redshift [OII] and [OIII] sources will be identified using photometric redshifts, while Ly α candidates using color-color [(H α -r) vs. H α] selections (Ouchi et al. 2008) or machine-learning codes that our team is developing.

WP1.5: Simulations and models (*Leads: K. Kraljic, F. Renaud, B. Vollmer*)

The observations will provide a complete, homogeneous dataset of star forming galaxies at different redshifts and HII regions in the MW. These data are an ideal testbed for the predictions of hydrodynamic cosmological simulations (IllustrisTNG: Springel et al. 2018; EAGLE: Shaye et al. 2015; RAMSES: Teyssier 2002; SIMBA: Dave et al. 2019), including those developed within the team (NewHorizon: Dubois et al. 2021), or semi-analytic models of galaxy evolution (Xie et al. 2025). The data will be used across a full range of scales and our goals include: the constraint of the star formation properties of galaxies as a function of halo mass (Boselli et al. 2023), the diffuse ionised gas emission of the intracluster component (Ahvazi et al. 2024), or made-to-measure magneto-hydro simulations of individual objects, from GMCs to galaxy scales (Renaud et al. 2014; Boselli et al. 2021, 2026; Vollmer et al. 2021) to study the evolution of feedback process on the gas dynamics and on the gas supply in galaxies. Simulations will also be used to study the role of magnetic field in confining the stripped gas, and the fate of the stripped material in the ICM.

Synergy of StarFEAST with other surveys: There is a clear synergy with the most important recent or future MW and extragalactic multifrequency surveys. X-rays data, characterizing the properties of the hot gas in massive haloes, are becoming available thanks to eROSITA, in addition to pointed observations from Chandra and XMM. The UV spectral domain (young stars) is available thanks to GALEX and UVIT archives, and might benefit from the future CASTOR space mission, with involved members of our team (Côté et al. 2025). Imaging data in the optical and near-IR spectral domain (bulk of the stellar emission), will be made available by surveys such as UNIONS (Gwyn et al. 2025), LSST, and Euclid. Spectroscopic observations are provided by SDSS or DESI (also taking into account future planned data releases). Mid- and far-IR data tracing the dust emission are available from WISE, Herschel and Spitzer programs (H-ATLAS, Eales et al. 2010; Hi-GAL Molinari et al. 2010). The radio domain (HI gas content and distribution, free-free and synchrotron emission, magnetic fields) has been covered by LOFAR (LoTSS; Shimwell et al. 2017) and GMRT (TGSS, Intema et al. 2017), or by targeted surveys such as Apertif at WSRT (Adams et al. 2022), or future SKA observations. The choice of fields with such great quality multifrequency data further boosts all our WPs and the legacy value of this large CFHT effort.

1.2 Scientific Goals of the POLU Survey

The second survey, POLU, covering an area of $\sim 4200 \text{ deg}^2$ in both galactic caps, will provide a detailed study of the $z > 2$ Universe. Imaging this footprint with two MB filters spanning $4000\text{--}4520\text{\AA}$ will allow the selection of ($2.3 < z < 2.7$) LAEs and ($2.7 < z < 3.4$) LBGs. POLU will join a coordinated effort among multiple telescopes, similarly to UNIONS, including the IBIS survey using the Dark Energy Camera on the Blanco telescope and the proposed Niji survey, using Hyper-SuprimeCam on the Subaru telescope, and a proposed survey using OmegaCam on the VST. The coordinated effort among CFHT, Blanco, Subaru and VST will cover $\sim 5000 \text{ deg}^2$ in a total of 5 MB filters from 4000\AA to 5300\AA .

Recently, the combination of four independent cosmological probes—baryon acoustic oscillations (BAO), the cosmic microwave background, supernovae, and weak lensing—has led to the surprising indication that DE may evolve over cosmic time. Although such evolution was not anticipated, it raises fundamental questions about the early behavior of DE

and its connection to primordial cosmology, highlighting the need for new high-redshift datasets capable of providing novel and robust constraints. In this context, these coordinated surveys will provide LAE and LBG targets for the second phase of the DESI instrument (DESI-II). Follow-up spectroscopy, beginning in 2029, will enable tests of primordial physics and place constraints on DE in the matter-dominated regime, where linear clustering applies and dynamical DE models yield distinct predictions. Even without spectroscopic follow-up, these two samples—comprising millions of LAEs and LBGs—enable robust studies of primordial non-Gaussianity through their angular auto-correlations and cross-correlations with CMB lensing. In addition, POLU will significantly improve photometric redshift estimates for future weak lensing surveys, such as those conducted by Rubin and Euclid. POLU will also initiate studies of dark matter within dwarf galaxies.

WP2.1 Dark Energy at $z > 2.0$ (*Leads: W. Percival, N. Palanque-Desabrouille*)

The BAO and Redshift Space Distortion (RSD) results from the DESI DR1 & DR2 analyses are indicative of a time-evolving (dynamic) DE (Adame et al. 2024, Abdul-Karim et al. 2025). These results have spurred a further exploration of the time history of DE, with explanations that include later-time thawing models or early-time, decaying DE models. A DESI-extension survey (2025–2028), in combination with supernova experiments, will explore the late-time (low-redshift) regime. This proposal aims to open a new window on the *higher*-redshift regime by identifying galaxy tracers of the large scale matter distribution and targeting these with DESI-II (starting in late 2029) to test the evolution of dynamical DE in the phase where its energy density is growing with time. MB imaging efficiently selects high-purity samples of LBGs and LAEs at redshifts $z > 2$. In POLU, we will use the two bluest filters of a set of five 260Å-wide filters spanning the *g*-band. LAEs and LBGs have been successfully identified from DECam imaging using these filters, with spectroscopic follow-up using DESI confirming $\sim 72\%$ redshift success rate in 30 minutes of integration (see Technical Justification Document), yielding number densities of $\sim 500 \text{ deg}^{-2}$ secured redshifts of LAEs and LBGs at $2.3 < z < 3.4$. We forecast that POLU plus the surveys mentioned above using the Blanco, Subaru, and VST telescopes, combined with spectroscopic redshifts from DESI-II, can measure the DE fraction in the redshift range $2.3 < z < 3.4$ with $\sim 2\%$ precision per redshift bin, which corresponds to a detection of $\Omega_{\text{DE}} \neq 0$ at better than 3σ at these redshifts (see Fig. 4), which is the first time this will have been achieved.

WP2.2 Physics of the Early Universe from 2D and 3D Clustering (*Leads: xxx, P. Zarrouk*)

An area that has clear potential for discovery of new physics lies in the residual signal from the early Universe that appears in large-scale structure today. POLU, along with DESI-II follow-up, will obtain precise clustering measurements that suffer far less processing of the density field relative to low redshift measurements. These measurements will offer a closer representation to the initial conditions imposed by inflation, and provide a step toward probing inflationary physics with large scale structure. One example of inflationary physics accessible to POLU is primordial non-Gaussianity which alters the expected power spectrum of dark matter haloes. This change causes a scale-dependent bias of the clustering of galaxies. As the deviation arises on very large scales, we need large survey volumes in order to beat down the uncertainty due to cosmic variance, best achieved by going to high redshifts. The LAEs and LBGs, in the redshift $2.0 < z < 3.5$ range, are the most distant matter tracers that are not dominated by shot noise. POLU is a unique survey in this redshift range that will select millions of LBGs and LAEs in the ($2.3 < z < 3.4$) redshift range. For studying primordial non-Gaussianity, we will use two complementary approaches. First, we will measure f_{NL} in the 3D power spectrum as illustrated in the right panel of Fig. 5, using DESI for the determination of the spectroscopic redshifts of the LBG and LAE samples. Secondly, we will use the angular power spectrum of the photometric sample (see left panel of Fig. 5) with the LAEs and LBGs. For a given footprint, this 2D approach is less sensitive than the 3D approach, but for extremely-large-scale clustering studies, much of the information on non-Gaussianity remains preserved (Slosar et al. 2008). In this way, we will be able to give a first f_{NL} measurement as soon as POLU is finished and before DESI-II starts in 2029. The 3D measurement will, of course, be more precise, but that will come later.

WP2.3 Cross-correlation science at $z > 2.0$ (*Leads: xxx, E. Chaussidon*)

The high- z galaxy survey we propose is uniquely constraining when combined with CMB lensing measurements from Planck, ACT and Simon Observatory (Galitzki et al. 2018). Cross-correlating the LAE and LBG samples with CMB lensing maps will provide a number of cosmological constraints that are currently limited by a lack of high-redshift galaxies with narrow, well-characterized redshift distributions. Indeed, CMB lensing can be measured to high- z , providing access to the underlying matter field without the need to model galaxy bias. Unfortunately CMB lensing alone mostly provides information that is projected along the line-of-sight (and with a broad redshift kernel). Cross-correlation with large scale structure (LSS) in several narrow ($\delta z \approx 0.2$, corresponding to a MB filter) redshift bins—CMB lensing tomography—can break the degeneracy with galaxy bias inherent in LSS alone and measure the amplitude of perturbations as a function of redshift. This provides tighter constraints on modified gravity (Pullen et al. 2015), neutrino masses (Yu et al. 2023), and

DE (Yu et al. 2022), while mitigating some of the possible systematics. At the same time, the cross-correlation of LSS with CMB lensing can potentially improve the robustness of constraints that rely on ultra-large scales, such as measurements of local non-Gaussianity. This method has already been successfully implemented with QSOs (Krolewski et al. 2024). We can safely extend it to our sample of galaxies, and it will already give a very accurate result before DESI-II starts up. Similarly, the cross correlation with CMB lensing will be able to provide σ_8 constraints of 2.8%, an order of magnitude tighter than previous studies at similar redshifts (Piccirilli et al. 2024).

WP2.4 Galaxy Evolution and Environment at Cosmic Noon (*Leads: xxx, J. Richard*)

POLU will identify millions of LAEs and LBGs and will be the largest extant sample of high- z galaxies (Mentuch Cooper et al. 2023). Since the bulk of LAEs are low-luminosity dwarf galaxies (similar to the LMC), and brighter LBGs are $\sim L^*$ galaxies (Reddy et al. 2009, Zhang et al. 2021), these data will enable an unprecedented study of the processes important for hierarchical galaxy formation at an epoch shortly before the peak in the star-formation rate density in the Universe (i.e., “cosmic noon”). POLU will also help to identify an unprecedented number of Ly α “Blobs”, large spatially extended (~ 50 -100 kpc) nebulae which mark the formation sites of groups of galaxies (Ramakrishnan et al. 2023, Steidel et al. 200). The ~ 40 Gpc³ volume covered by the combination of POLU and IBIS surveys will yield \approx protoclusters at $M_{\text{halo}} > 10^{15} M_{\odot}$ (i.e., Coma progenitors), providing the best opportunity of detecting the most massive systems at these redshifts. In comparison, existing NB surveys at comparable redshift jointly cover $\sim 1/50$ th the volume of our proposed survey (Lee et al., 2024). As a result of the DESI-II spectroscopic follow-up, we will be able to study the gas metallicity, dust reddening and stellar ages in these galactic building blocks as functions of local environment, star-formation rates, Ly α escape fraction, large-scale clustering, and redshift with unprecedented precision (Reddy et al. 2022). Specifically selecting the largest overdensities of LAEs and LBGs will allow us to identify the most suitable regions with gas filaments forming the cosmic web, one of the most fundamental predictions of Λ CDM (Bacon et al. 2021; Fig. 6). Direct imaging of these gaseous filaments in Ly α emission will be within reach of the VLT/BlueMUSE instrument (Richard et al. 2019) thanks to the cosmological surface brightness enhancement compared to MUSE, while simultaneously probing the CGM emission properties of individual LAEs and LBGs (see Fig. 6). The unique set of data provided by POLU will thus be ideally suited to link similar studies of the local and the high- z Universe ($z=4.5$) done within the StarFEAST project.

WP2.5 Photometric Redshifts and Dwarf Galaxies at $z < 0.4$ (*Leads: xxx, yyy*)

Even with the new generation of wide-field multi-object spectrographs, redshift surveys only capture a small fraction of galaxies detected in imaging. Consequently, cosmological assessments relying on weak lensing, such as those planned by Rubin/LSST and Euclid, heavily depend on accurate photometric redshifts. Moreover, precise photometric redshifts are crucial for identifying the hosts of transient phenomena like LIGO events. The two MB imaging surveys (two bands with POLU and three bands with IBIS) will significantly enhance the accuracy and purity of photometric redshifts compared to conventional methods that rely solely on broad-band photometry. To illustrate the advantage of using MB filters for photo- z , we have considered dwarf galaxies which offer a powerful probe of small-scale structures, dark matter, and the galaxy-halo connection. Galaxy-galaxy lensing is a powerful way to directly probe to the edges of dark matter halos. Wide and deep field imaging surveys like LSST, Euclid, and Roman will image large numbers of low-mass dwarf galaxies, transforming our understanding of dark matter and galaxy formation at the lowest mass end. However, the main limitation to measuring their dark matter halo profiles is not the lensing signal-to-noise from these surveys, but rather the ability to obtain accurate redshifts for the dwarf galaxy lenses (Leauthaud et al. 2020, Luo et al. 2024). By combining our MB observations with broad-band photometry from Rubin, we will achieve a photometric redshift precision of $\sigma_{\Delta z/(1+z)} \approx 0.01$ and a catastrophic failure fraction of $\eta \approx 0.45\%$ to $r \sim 24$ (see Fig. 7). With a 5000 deg² footprint we will identify ~ 10 M dwarf galaxies with $8.0 < \log M_*/M_{\odot} < 9.0$ at $z < 0.4$. Such high quality lensing measurements will allow us to constrain the dark matter halo profiles of dwarfs, and thus allow us to distinguish different dark matter models (e.g., CDM vs. self-interacting DM).

2. Suitability of CFHT

Long known for its outstanding imaging capabilities, the MegaCam instrument has largely been outpaced by larger facilities, e.g. the 8-10m class telescopes (Subaru, LSST) or space-based facilities, (Euclid, Roman), particularly for broad-band imaging. Indeed, for the g -band, taking into account the different fields of view, telescope diameters, and the time between exposures, the LSST is 25 times faster than the CFHT. Only a few wide field cameras, however, are equipped with MB and NB filters. This CS imaging project is thus a unique and powerful capability of CFHT. On the one hand, the VESTIGE project has clearly demonstrated the feasibility and success of such a program; on the other hand, a wide survey like DECaLS (Dey et al. 2019), developed specifically for DESI, has generated more than 2000 citations for the Blanco Telescope. Thus, the legacy value of this CS is undoubtedly very high and the data will be a reference for years to come.

3. Risk assessment

The observing strategy and scientific exploitation of the proposed program have been optimised to limit the project risks, while maximising the scientific return. In particular, the most significant risk mitigation comes from the experience of the team with similar NB and MB observations (e.g. the VESTIGE and IBIS surveys) or the leadership and ownership of simulation suites required to reach the proposed goals.

Risk 1: Poor weather conditions. MEDIUM risk (Probability: 3/5, Impact: 2/5) All ground-based instruments are at risk from poorer than average weather conditions, limiting the survey progress and efficiency. For both SRFEnv and POLU, we mitigate this effect with a complete RA distribution of the targets, making them observable in both semesters, and by a large variety of targets, some of which requiring less stringent conditions (MW and LG). By acquiring data in multiple epochs, we will average out seeing, sky darkness, and transparency conditions, reducing the magnitude of the risk compared to single pass surveys. In addition, the two surveys do not require the same observing conditions (grey/dark sky and seeing), which makes the survey much more flexible and less sensitive to weather conditions.

Risk 2: Instrument failures and reduced completion rate. LOW risk (Probability 2/5, Impact: 2/5) The CFHT/Megacam has proven to be a reliable machine, however, with aging, it is possible that the rate of failures will increase. For SRFEnv Survey, we have designed a prioritisation strategy to cover the widest range of environments in year 1, to grant the scientific success of the survey in case the full program will not be completed. In case of a 75% completion rate, a large fraction of the expected results will be reached although with a lower statistical significance. Shallower or aperture limited data exists in the Galactic plane or for local galaxies, which can be ingested in our dataset, at the expenses of homogeneity, in case the completion rate is significantly below our targets for these specific WPs. For POLU, if we will not be able to cover the planned 4200 deg² area at the planned depth with the two bands, there are three ways to mitigate the effect: a) reduce the surface area b) reduce the depth (i.e., exposure time per pointing) c) remove one of the two bands. Since we want to maintain a consistent number of selected targets throughout the survey, we cannot change the depth during the survey. This decision can only be made at the outset. Therefore, it is very likely that we will reduce the size of the footprint in coordination with IBIS, which observes the reddest bands.

Risk 3: One or more WP leads leave the consortium. LOW risk (Probability 2/5, Impact: 1/5) While it is possible that one or more WP leads cannot commit the time initially planned to the project, our management scheme has 2/3 co-leads for each WP and our team is large enough that new people can take these leadership roles. These actions significantly mitigate the impact of this risk. In the specific case of POLU, since the scientific program is directly linked to that conducted with DESI-II and DESI-II has more than 200 active researchers, it will be easy to find replacements.

4. Synergies within this CS proposal

There is an obvious synergy between the two surveys of this CS proposal, e.g. the study of the environmentally driven galaxy formation and the identification of LAEs and LBGs at $2.2 < z < 3.2$ through NB and MB imaging. Indeed, although limited on a much smaller area, NB observations in the H α filter will detect LAEs at $z \simeq 4.5$, thus enabling studies similar to those proposed by POLU at higher redshift. The overlapping regions between POLU and StarFEAST covers at least 30 deg², that summed to the one mapped by VESTIGE (100 deg²), will provide a large area (130 deg²) covered by NB, MB and broad-band filters, plus follow-up spectroscopy with DESI, enabling new science goals across a significant volume and redshift. Specifically, this collaboration will likely provide additional high- z targets for DESI spectroscopy to further constrain the large scale structure of the cosmic web and the properties of the embedded galaxies. Moreover, DESI data releases will provide an excellent coverage of the galaxies in a large range of environments to constrain their dust attenuation, metallicity, ionisation parameters, further enabling the goals of WP1.3.

Besides the direct synergies, the POLU and StarFEAST surveys have also clear complementarities which significantly strengthen the overall legacy and immediate science return. The observations of POLU are part of a wider effort involving several ground-based facilities (DESI at the Mayall telescope, DECam at the Blanco telescope) of interest for a large international community. This will grant a high international visibility with an expected high citation rate for the associated publications, with CFHT being one of the partners, and the main publication outcome will come when a significant fraction of the observations have been taken. StarFEAST, on the other hand, is planned to deliver a high publication rate starting early in the project phase, with a clear visibility for the CFHT in the international astronomical community but also for the general public through outreach projects (e.g. spectacular images of resolved galaxies). StarFEAST is also planning part of the observations in brighter sky conditions, therefore maximizing the overall efficiency of the combined CS.

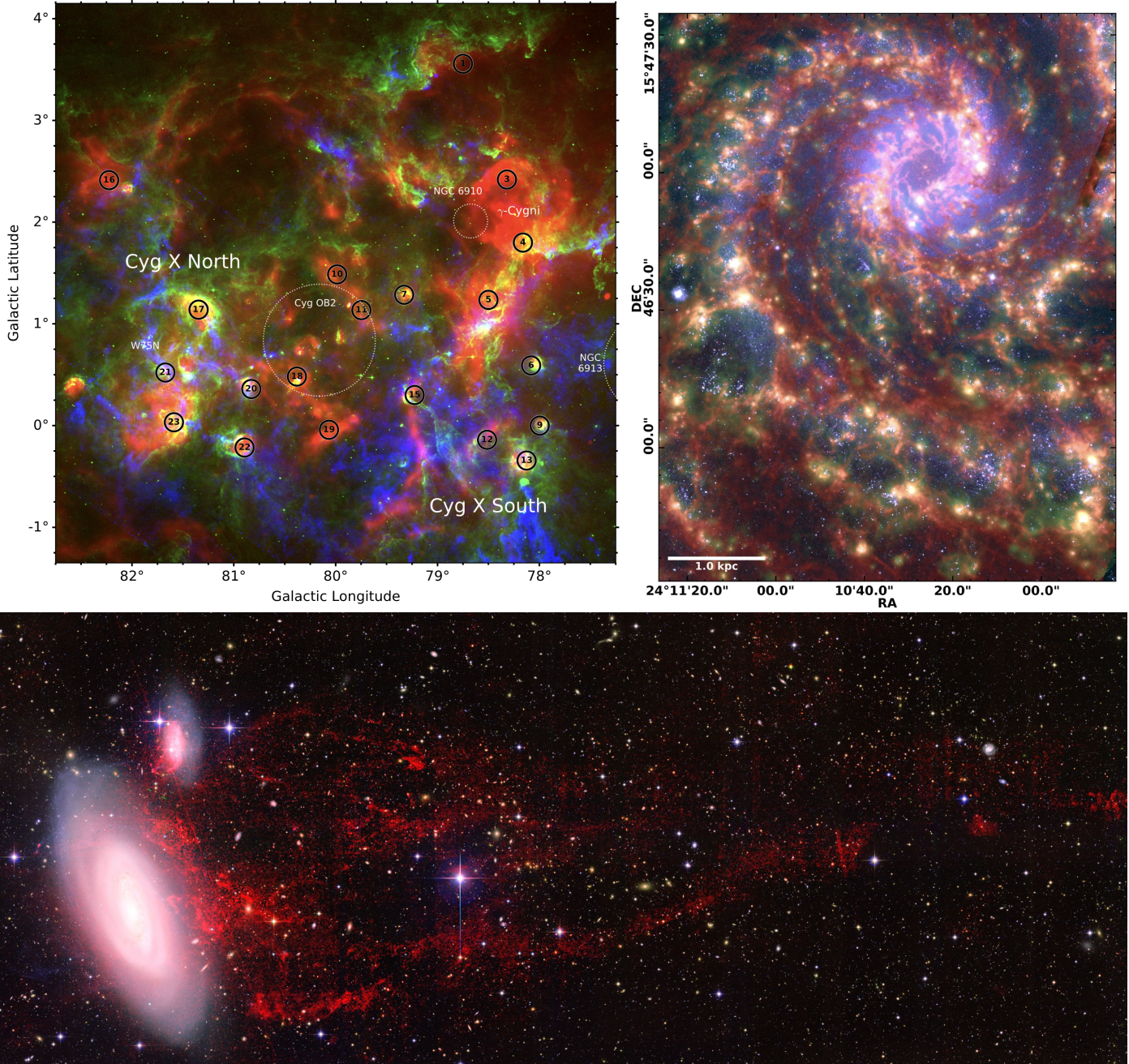


Figure 1. Upper left: Colour image (red: 1.4 GHz continuum; green: $8\mu\text{m}$ PHAs emission; blue: $^{13}\text{CO}(1-0)$ molecular gas) of the Cygnus X star forming complex in the MW (Emig et al. 2025). The OB (star forming) associations (black circles) are interacting with the surrounding ISM (gas and dust) via stellar feedback, modifying the distribution, density, and temperature of the gas needed to feed star formation. Upper right: Colour image of the galaxy NGC 628 (red: MIRI F770W, green: MUSE $\text{H}\alpha$, blue: B -band HST; Watkins et al. 2023). Bubbles formed by stellar winds have strong effects on the surrounding ISM, modulating galactic flows which regulate the star formation process globally. Lower panel: Colour image of the massive spiral galaxy NGC 4569 in the Virgo cluster. The red colour shows the ionised gas emission as derived from the $\text{H}\alpha$ NB imaging data gathered at the CFHT during the VESTIGE survey ($\Sigma(\text{H}\alpha) \simeq 2\text{--}4 \times 10^{-18} \text{ erg s}^{-1} \text{ cm}^{-2} \text{ arcsec}^{-2}$). The long filamentary structure escaping from the galaxy disc to the west is ionised gas stripped from the galaxy during its hydrodynamic interaction (ram pressure) with the surrounding hot ICM. We expect to detect similar structures in perturbed galaxies in groups and clusters located within the GW and the PPS.

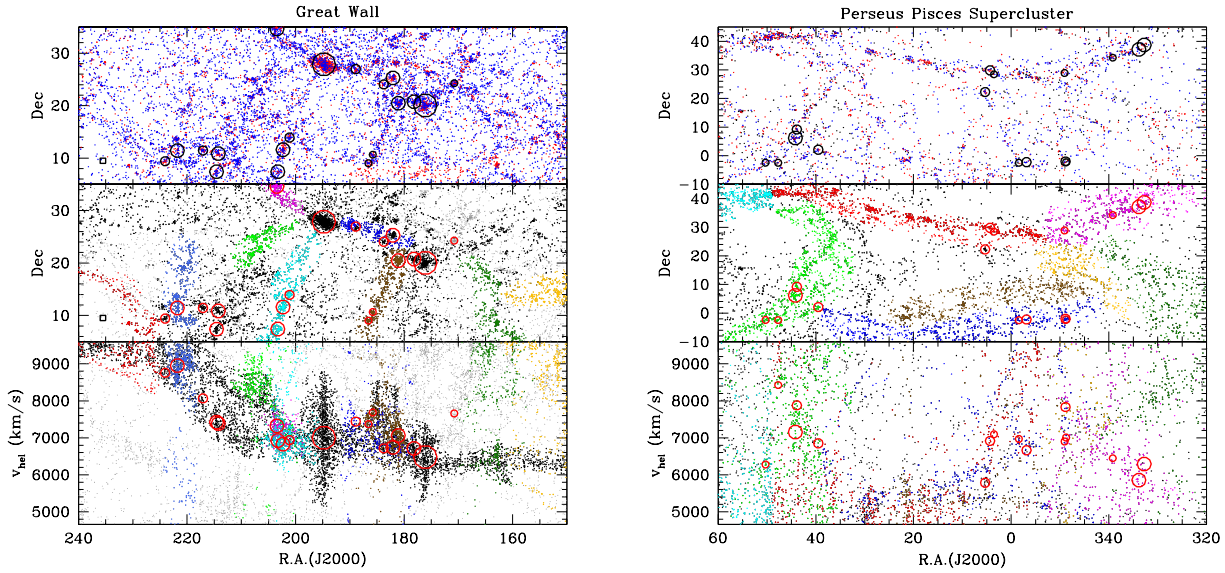


Figure 2. Distribution of galaxies at $4660 < v_{hel} < 9600$ km/s covering the range of the H α 9604 NB filter in the GW (left) and PPS (right) regions. Upper panel: sky distribution of star forming (blue) and quiescent (red) objects. Black circles indicate the high-density regions with a mean recessional velocity $v_{hel} \pm 3\sigma$ within the filter velocity range, with size depending on their halo mass which ranges within $10^{13} < M_{halo} < 10^{15} M_{\odot}$. The massive clusters at $RA \sim 178^{\circ}$ and $RA \sim 195^{\circ}$ are A1367 and Coma (A1656), the dense region at $RA \sim 50^{\circ}$ and $Dec \sim 40^{\circ}$ in the right panel is Perseus, which we will not target since it includes galaxies outside the filter range. The black box in the lower left corner is the MegaCam (1 deg^2) FoV. Central panel: same sky distribution but color coded for the galaxy filament membership. Lower panel: RA vs. recessional velocity distribution for galaxies in the declination range $5^{\circ} < Dec < 35^{\circ}$ (GW) and $-10^{\circ} < Dec < 45^{\circ}$ (PPS) chosen for the present survey. The GW (left) structure stretches between $\sim 150^{\circ} < RA < \sim 240^{\circ}$ and $6500 < v_{hel} < 9500$ km/s. The selected high-density regions are marked with red circles. The most massive of them show the characteristic finger of God signature due to their high velocity dispersion. Galaxies are color coded as in the middle panels.

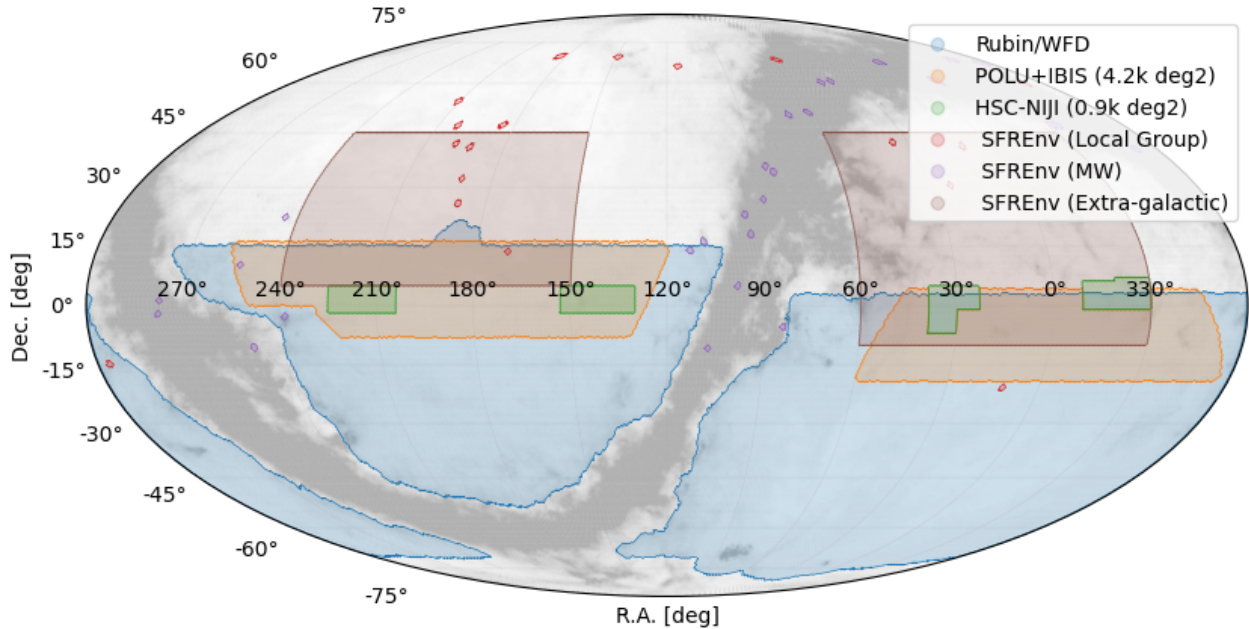
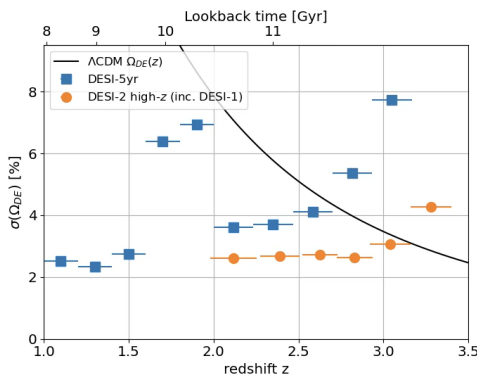


Figure 3. Footprint of the POLU survey (orange boxes), shown in comparison to the footprints of the Rubin/LSST (blue). The grey background shows the Galactic dust. The POLU footprint is split into two equatorial fields in the NGC and SGC (observable during the A and B semesters, respectively) and designed to maximise overlap with data from the other surveys. Footprint of the StarFEAST Survey: sky distribution of Galactic star forming regions (purple circles), Local Galaxies (red circles) and local Large Scale Structures, the filamentary structures easily identifiable within the brown rectangles.



gaCam CFHT CS – StarFEAST and POLU

Figure 4. The expected precision on Ω_{DE} for the planned DESI-II survey (orange dots), which requires the targeting data proposed with POLU, compared with the completed DESI 5-year survey (blue). The proposed imaging (and subsequent DESI-II follow-up) survey will provide the strongest constraints on Ω_{DE} at these redshifts for the next decade.

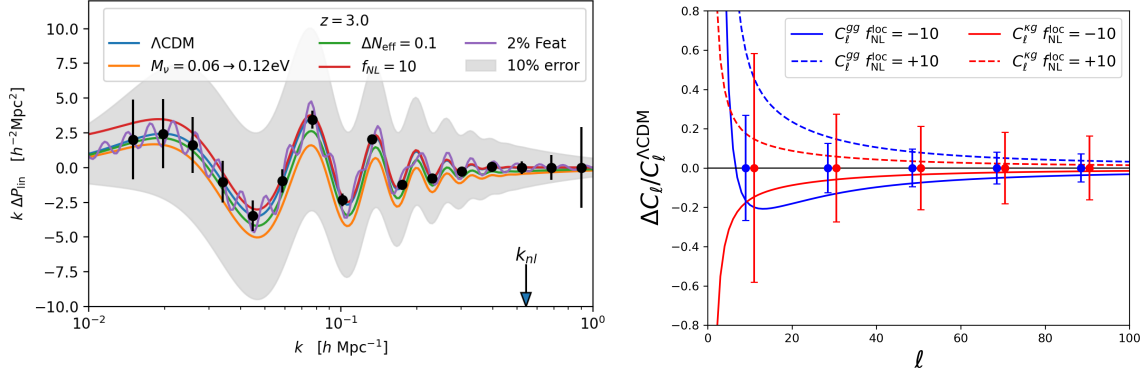


Figure 5. **Left:** 3D power spectrum of LBG and LAE samples in the $2.3 < z < 3.4$ redshift range. The fiducial model (ACDM) assumes a summed neutrino mass of 60 meV, while the other curves represent modifications such as a 120 meV neutrino mass, additional relativistic species (ΔN_{eff}), primordial non-Gaussianity of the local form (f_{NL}), and primordial features. **Right:** 2D angular power spectrum of LBGs and LAEs for $f_{\text{NL}} = -10, 10$; in blue the auto-correlation and in red the cross-correlation with CMB lensing.

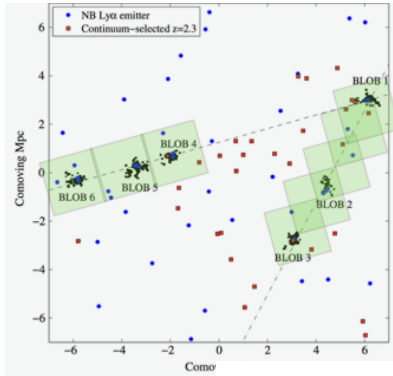


Figure 6. Illustration of overdense regions that can be identified with POLU thanks to the combination of continuum and line detections (background figure from (Erb et al. 20211)). Overdense regions of bright LAEs are identified as ‘blobs’ and are expected to be connected through gaseous filaments (dotted lines). Follow-up with VLT/BlueMUSE (green squares, through mosaicing) will allow us to directly image the diffuse IGM and CGM of these filaments that so far has been difficult to observe in emission.

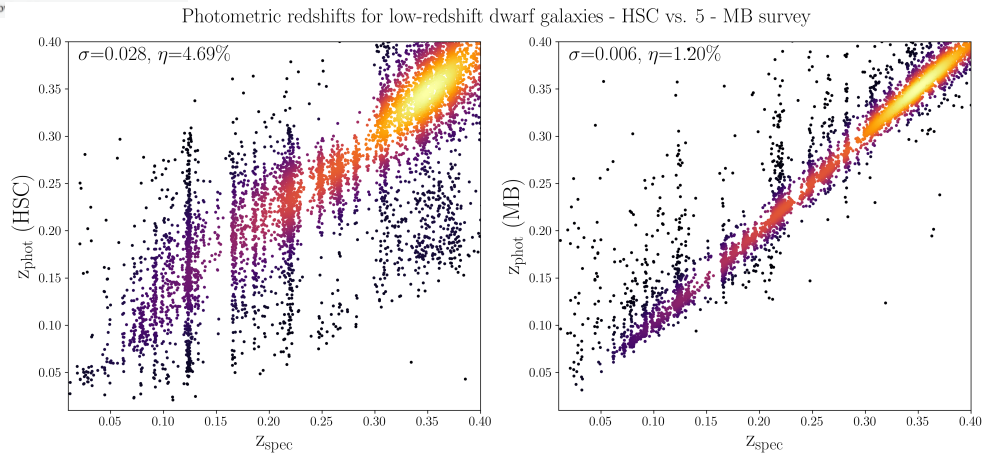


Figure 7. **Left:** Photometric redshifts for low-redshift galaxies computed using only broad-band *grizy* data from Subaru/HSC. **Right:** Photometric redshifts derived by including medium-bands. Adding the medium-bands results in “precision” photometric redshifts for low-redshift sources enabling faint dwarf galaxies to be identified, their dark matter halos to be studied via lensing, and their detailed spatial distribution within large-scale structure to be better characterised.

Technical justification

1. Design of the Community Survey

1.1 WP-SD: Design of the StarFEAST Survey

1.1.1 SD1.1: Selected sample

Milky Way. To sample the widest possible range in the parameter space required to reach our science goal (study the impact of early radiative feedback from high-mass stars on star formation properties), we selected 20 (essential) to 24 (desirable) star-forming complexes within the MW with different star formation rate, age, metallicity, gas and dust content, Galactic latitude, evolution stage of the ionised region, and strength of the ionising radiation. Furthermore, we are interested in sampling the interface between the ionised region and the photodissociation region. This requires the high sensitivity to LSB that can be achieved with MegaCam. The selected regions are located at all RAs and have $\text{Dec} > -15^\circ$ (Fig. T1), thus they are easily accessible from the CFHT. Twenty sources are the minimum number required to achieve sufficient statistics to reach our scientific goals. Should the weather conditions not be favorable for the extragalactic surveys, a wider sampling of the selected regions and a few extra targets could be added to increase the sample. We checked whether similar data were available from NB imaging surveys such as VPHAS+ (VST, Drew et al. 2014) and IPHAS (INT, Drew et al. 2005). These surveys used 2.5 m telescopes to cover the Galactic plane with 360s exposures. Using MegaCam, we gain factors of 2 for the mirror area and 10 in integration time, reaching a $\text{mag}=23.5$ in the NB filter, vs. $\text{mag}=20$ in VPHAS+ and IPHAS for point sources. This turns into deeper sensitivities for extended features which are required to study the interface between ionised, neutral and molecular gas. Some of our selected primary sources have been partly covered with SITELLE. This will enable us to cross-calibrate the MegaCam data using spectroscopic measurements. Furthermore, the availability of multi-wavelength and multi-scale data on the selected sources enables in-depth analysis of the physics of early radiative feedback. The primary sample of 20 sources covers 64 deg^2 and will be observed in three NB and in the g and r filters for a total of 3.87 h/deg^2 . Considering an observing time of 5h per night, this program requires **250h equivalent to 50 nights**.

Local Galaxies: The LG sample includes all the star-forming objects with $\text{Dec} > -30^\circ$, radius $R_{W1} > 7.5 \text{ arcmin}$ in the WISE large galaxy catalogue of Jarrett et al. (2019) and $A_V < 1.0 \text{ mag}$ (18 galaxies). Given their large angular size, which can hardly be covered with IFU spectrographs with FoVs generally limited in angular size (with the exception of SITELLE, which has a FoV of $11 \times 11 \text{ arcmin}^2$, others such as MUSE, PMAS, or MaNGA have a FoV of only $\sim 1 \text{ arcmin}^2$), these are ideal targets for pointed NB imaging. They requires 27 pointings in the 3 NB filters and 2 broad g - and r -bands with integration times similar to those proposed for MW HII regions for a total (including overheads) of **105h or 21 observing nights**. A few galaxies have (mainly $\text{H}\alpha$) NB imaging in the literature (Massey et al. 2006), others have been partly mapped with IFU spectrographs (e.g. SIGNALS). This survey will provide for the first time a unique, homogeneous, and complete sample with an unprecedented sensitivity in the $\text{H}\alpha$, [SII], and [OIII] lines suitable for statistical studies.

Large scale structures: The GW and the PPS extend over several thousands of deg^2 and cannot be blindly mapped over their full extension. The GW is located in the region $8\text{h} < \text{RA} < 17\text{h}$; $5^\circ < \text{Dec} < 44^\circ$, while the PPS in $21\text{h} < \text{RA} < 5\text{h}$; $25^\circ < \text{Dec} < 45^\circ$ (Fig.2). The GW and PPS are clearly identified as a network of filaments connecting massive nodes of the cosmic web. To probe the full range of environments we therefore need to target massive haloes (groups and clusters) as well as filament-like structures. Regarding groups and clusters, in the GW (spanning the range $\approx 6500 < cz < 9000 \text{ km/s}$) we select them from the catalogue of Wilman et al. (2010), where we found 19 high-density regions with halo mass $10^{13} < M_{\text{halo}} < 10^{15} M_\odot$ and $cz \pm 3\sigma$ within the filter transmission curve (Fig. 8). Two of them have a halo mass $M_{\text{halo}} > 10^{14} M_\odot$ (Coma, A1367) and have the characteristic finger of God shape due to their high velocity dispersion ($\sim 1000 \text{ km/s}$). Although with a lower density, due to the limited depth of the 2MASS redshift survey (Huchra et al. 2012), similarly massive haloes can be found in the PPS sky region, where we identified 16 target groups. The catalogued star forming galaxies (blue dots) located within the selected high-density regions are ~ 1500 , and the sample size becomes $\sim 3000 - 4000$ galaxies once early-type systems are included. These high-density regions will be mapped using mosaicked MegaCam fields, with the mosaic size selected as a function of the angular extension of the target groups. These mosaics range from 4×4 for the most massive clusters down to single pointings for the low mass systems for a total of 197 pointings. This tiling strategy covers up to $\sim 2r_{200}$ of the target groups, including the infalling regions outside of r_{200} where environmental perturbations are starting to become important. Filaments of galaxies are also selected within these regions. We select the structures with an overdensity (compared to the mean galaxy density) at the filament spine $\delta > 5$ and we grow the selection to adjacent galaxies until the average overdensity for each filament is $\delta > 3$ (the lowest density regions will be used as reference sample). Filaments selected in this way are highlighted in different colours in the middle panels

of Fig. 2. Given the higher fraction of star forming galaxies in these environments, compared to clusters and groups, we will have at least ~ 10 star forming galaxies deg^2 . These numbers are lower limits since they correspond to the number of star-forming galaxies with an available redshift down to the SDSS limiting magnitude $r < 17.7$. We expect to detect weaker sources whose membership to the GW and PPS will be secured by the presence of the $\text{H}\alpha$ line emission within the NB filter. 200 selected fields will be used to map representative regions of 20 different filaments (with a mean of ≈ 10 gal/field). This will secure the detection of $\gtrsim 2000$ star forming systems, a number comparable to the one reached for the massive haloes and suitable to obtain the same statistical significance on a comparative analysis. The study of environmental effects on galaxy evolution involves a multi-dimensional parameter space, the large number of targets ($\gtrsim 3500$ in total) is necessary to split the sample in 4–5 bins of halo mass ($10^{13} < M_{\text{halo}} < 10^{15} M_{\odot}$, or overdensity $1 \lesssim \delta \lesssim 100$), galaxy mass ($10^7 < M_{\text{star}} < 10^{11}$), distance from group/cluster core ($0 < r/r_{200} < 10$) or position in the filament, while retaining at least 25 galaxies per bin to ensure a $\text{SNR} \approx 5$ on our measurements in each bin, assuming Poisson statistics. Indeed, all the physical variables regulating environmental effects strongly evolve from filaments to groups and to massive clusters: for instance, RPS depends on the galaxy velocity in the halo potential and the IGM density, starvation occurs before or near the halo virial radius. Moreover, the properties of galaxies are regulated by their own potential, often traced via their stellar (+gas) mass. The need for such a number of galaxies is therefore justified by the need to break the covariance among all these parameters. We therefore request 397 pointings, 197 for groups and clusters, 200 for filaments. Assuming 10,080s per pointing including overheads, and that archival broad-band imaging exists for a fraction of the footprint, we will require **995h equivalent to 199 nights**.

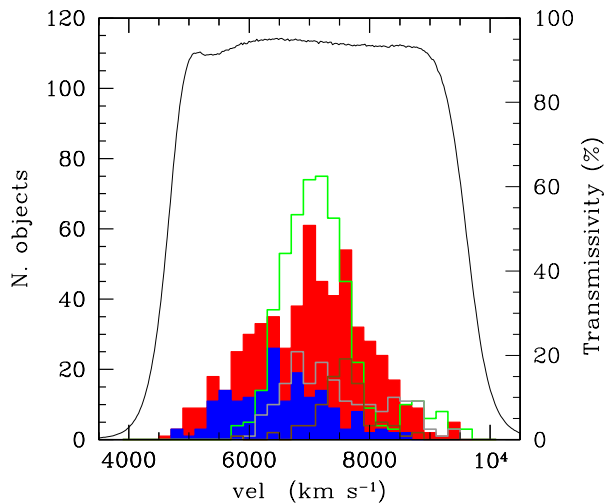


Figure 8. Velocity distribution of galaxies in Coma (red histogram), A1367 (blue), and in the selected groups of mass $5 \times 10^{13} < M_{\text{halo}} < 10^{14} M_{\odot}$ (green), $2 \times 10^{13} < M_{\text{halo}} < 5 \times 10^{13} M_{\odot}$ (grey), and $M_{\text{halo}} < 2 \times 10^{13} M_{\odot}$ (brown). They are all within the plateau of the maximum transmissivity of the 9604 $\text{H}\alpha$ Off filter selected for this survey. This is also the case for galaxies belonging to the selected filaments (see Fig. 2, lower panel).

1.1.2 SD1.2: Integration times.

We propose to survey different representative structures using MegaCam coupled with three NB filters $\simeq 100 \text{ \AA}$ wide and available at the CFHT: 9603 ($\text{H}\alpha$; $\lambda=6591\text{\AA}$; $\Delta\lambda=106\text{\AA}$; $T=93\%$), 9604 ($\text{H}\alpha$ Off; $\lambda=6719\text{\AA}$; $\Delta\lambda=109\text{\AA}$; $T=95\%$), and 9501 ([OIII]; $\lambda=5007\text{\AA}$; $\Delta\lambda=102\text{\AA}$; $T=91\%$). The $\text{H}\alpha$ and [OIII] filters are designed to observe these lines at rest frame, and will be used for MW and LG systems. The $\text{H}\alpha$ -Off filter is sensitive to the rest frame emission of the [SII] doublet, and will thus be used for the same targets. It is also sensitive to the $\text{H}\alpha$ emission of galaxies with $+4660 < v_{\text{hel}} < +9600$ km/s, the range of the selected structures (Fig. 2 and 8). *The large FoV of the camera (1 deg²), combined with the high end-to-end throughput of the telescope and camera, and the excellent imaging quality of the telescope, make CFHT the best instrument available to the international community for this programme.*

Two different observing strategies will be used for MW and LG targets vs the other extragalactic ones. One of the goals of our program is the detection of LSB features frequently observed in nearby cluster galaxies (e.g. Yagi et al. 2010) or predicted by hydrodynamic simulations (e.g. Tonnesen & Bryan 2010). Such features have a typical surface brightness of $\Sigma(\text{H}\alpha) \simeq 2 \times 10^{-18} \text{ erg s}^{-1} \text{ cm}^{-2} \text{ arcsec}^{-2}$. Similar surface brightnesses must be reached to measure a possible truncation in the $\text{H}\alpha$ distribution (harassment) or faint and fading discs predicted by starvation scenarios. These values are $\sim 60\times$ fainter than those reached in previous $\text{H}\alpha$ NB observations of galaxies in the GW using 2m class telescopes (Gavazzi et al. 2013) and have angular sizes of several arcmin at the distance of this structure (~ 100 Mpc). The $\text{H}\alpha$ observations carried out at the CFHT during the VESTIGE survey (using the MP9603 filter) have shown that these SB limits can be reached in 7200s, and after rebinning the data to $2.8''/\text{pixel}$, provided that the data are acquired and reduced using the Elixir-LSB pipeline in dark sky conditions. The point source sensitivity is $F(\text{H}\alpha) \sim 4 \times 10^{-17} \text{ erg s}^{-1} \text{ cm}^{-2}$ (5σ), sufficient to detect

the bright end of the LF of Ly α emitters at $z=4.5$ (Sobral et al. 2018, Tornotti et al. priv. comm.). Given the negligible differences in the MP9603 and MP9604 filters ($\pm 3\%$ in band width and 2% in throughput), we estimate these forecasts will be highly accurate for the proposed observations. For the determination and the subtraction of the stellar continuum we will use a combination of the broad-band r and g filters, which is necessary for an accurate sampling of the intrinsic colour of the observed targets (Boselli et al. 2018a). This is particularly important in the inner regions of bright early-type galaxies, which are bright and with rapidly changing colours with radius (age and metallicity effects). These 2 broad-band filters are $\sim 14x$ wider than the H α filter, so the integration time scales accordingly (720s in each band). The broad-band data should be taken with similar weather constraints (seeing and background illumination) as the H α frames to minimize flat fielding residuals that could negatively impact the identification of LSB features. With a total integration of 720s in the r -band and 720s in the g -band we will reach a limiting magnitude of $r = 24.5$ AB mag (5σ). To summarize, each of our extragalactic field requires 7200s integration in H α , and 720s integration in the r - and g -bands each, for a total of 8640s per survey tile. Each exposure in the 3 filters, will be divided in 12 exposures (600s for H α and 60s for g and r) optimally dithered to cover the CCD gaps and minimise the possible contamination from the reflections of bright stars. The dithering pattern will be optimised for both contiguous regions within extended structures such as massive clusters, and in more isolated pointings, with procedures developed by our team. Galactic star-forming regions and LG are much brighter and thus require shorter integration times to avoid saturation. We plan to observe them using 12 exposures 300s long for the 3 NB filters and 30s for the r and g filters. The corresponding total integration time per pointing is 11,520s. These regions are extended several deg 2 on the sky, and thus require ad-hoc mapping as done for the extragalactic sources.

1.1.3 SD1.3: LSB Observing Strategy.

The observing strategy is driven by our scientific goals requiring the LSB observing technique to map faint extended features. We will use the Elixir-LSB pointing strategy successfully developed for VESTIGE and NGVS (Ferrarese et al. 2012). The strategy requires an uninterrupted sequence of 6 single exposures to be acquired in an observing group (OG). A large dither strategy, optimised for the LSB mode, will be adopted to cover the gap between the CCDs and to model the sky background even in the presence of extended sources in the each exposure, a goal that cannot be reached with filtering based sky subtraction techniques. Our integration times ensure each exposure is background limited even when the moon is below the horizon, a key requirement of the LSB data reduction pipelines. Calibration of the g - and r -band data will use standard MegaCam/MegaPipe procedures based on stellar photometry from external catalogues (e.g. PS1). For the NB filters we will follow the same procedure successfully used for VESTIGE: i.e., the NB frames are calibrated using colour corrected magnitudes for the stars in the field and then a pure line emission image is generated using a colour-dependent correction for the stellar continuum using the g - and r -band data. This technique has been proved to reach accuracies of $<3\%$ when compared to spectroscopic MUSE data (e.g. Boselli et al. 2021).

Targets are uniformly distributed at all RAs, and are thus observable any time during the year, maximising scheduling flexibility (Fig. 2). The fields will be prioritised in such a way to ensure maximum scientific return as the survey evolves. Considering 40s of overhead/exposure, this leads to 10080s of telescope time per extragalactic field ($12 \times 600s + 12 \times 40s$ for H α , $(12 \times 60s + 12 \times 40s) \times 2$ for g and r) and 13,920s per LG and MW sources ($12 \times 300s + 12 \times 40s$ for H α , [OIII], [SII] plus $(12 \times 30s + 12 \times 40s) \times 2$ for g and r). The MW regions we propose to observe covers 65 deg 2 , the LG 27 deg 2 , while the extragalactic fields ~ 400 deg 2 . To be completed, the survey requires 1350h, or assuming a success rate of 5h/night for MegaCam, 270 nights of observations (50 for MW, 21 for LG, 199 for the extragalactic sources, equally shared between the GW and the PPS). In summary, **the total request for the StarFEAST WP is 270 nights, 65 in grey time and 205 in dark time (see sky conditions).**

1.1.4 SD1.4 Sky Conditions.

Given the extended, LSB nature of the ionised gas tails, data for this survey can be gathered in standard CFHT seeing conditions, often occurring at Mauna Kea ($\leq 1.0''$, with 20% tolerance). Taking the VESTIGE survey as a reference, these constraints lead to a mean H α seeing of 0.73 arcsec. We assume this value to make forecasts on the limiting luminosity of point sources required by the high- z galaxies WP. Due to their large sky extension, Galactic sources can be observed even in poorer seeing conditions (up to $\sim 1.5-2''$). NB H α observations of extragalactic fields are required to detect faint extended emission features. Our exposure time calculations assume dark sky conditions (Fraction of Lunar Illumination, FLI <0.1) or moon below the horizon. Based on the analysis of the VESTIGE images and using the ESO skycalc tool with the Mauna Kea site parameters, we estimate that the exposure times would increase by 35% if the mean FLI is 0.2 or by 100% if the mean FLI is 0.4. As a result, these observations are more efficiently scheduled in dark or moderately grey conditions such that the mean FLI of the 12 visits of each pointing in the sky is $\langle \text{FLI} \rangle \sim 0.1$. We also require a minimum

moon-target distance of 50 deg. Similar considerations can be made for the g -band and [OIII] NB observations, which are best scheduled in dark conditions. All r -band data, and $H\alpha$ data of MW and LG targets can be gathered in grey time, up to a FLI = 0.4. Observations can be gathered with a moderate < 0.2 mag extinction under thin cirrus, provided that cloudy sky observations are obtained in dark time to avoid light scattering from a significantly illuminated moon. *The 270 nights requested for the StarFEAST program have been estimated using these sky conditions. In case the observations will be gathered in worse seeing and darkness conditions, the total number of nights should be increased accordingly.*

1.1.5 SD1.5 Best use of available data.

Broad-band r and g imaging data are partially available for the surveyed regions. We plan to use them whenever their quality in terms of sensitivity, uniform illumination, and image quality, grants the best exploitation of the NB imaging data gathered during this survey. These mainly concern the areas covered by the extragalactic pointings thanks to UNIONS (Gwyn et al. 2025) in the GW region for $\text{Dec} > 30^\circ$ and with a patchy coverage in the range $23^\circ < \text{Dec} < 35^\circ$ in the PPS region (Mondelin et al. 2026), and thus have a limited overlap with the proposed observations (Fig. 2). Similar CFHT data are also available for a few LG. Gathered at the CFHT with similar seeing conditions, r -band data reach $r=24.2$ mag vs. $r=24.4$ for our survey (10σ in a 2 arcsec aperture) and, whenever available, will be used without any extra observation. UNIONS g -band data come from the Subaru WHIGS survey, and reach $g=24.54$ mag vs. $g=24.92$ mag for our survey. An extra exposure of 340s might be necessary to reach the same sensitivity, but we will do that after testing it if necessary. The overlap with POLU, which provides imaging data in the blue, is limited only to $\sim 30\text{deg}^2$. These data will also be used whenever available.

1.2 WP-SD: Design of the POLU survey

1.2.1 SD2.1: Target selection of LAE and LBG

We will select Ly- α Emitters (LAE) targets with line fluxes of $F(\text{Ly}\alpha) \geq \sim 1.5 \times 10^{-16} \text{ erg s}^{-1} \text{ cm}^{-2}$ and Lyman Break Galaxies (LBG) targets at $r \leq 24.3$ AB mag, with two complementary strategies, using two medium bands, MB1, 4000 – 4260Å and MB2, 4260 – 4520Å, in combination with existing deep broad-band imaging from Rubin/LSST.

LAEs are young, star-forming galaxies that exhibit strong Ly- α lines in their spectra, often with relatively weak continuum emission. Their strong emission lines also offer a high contrast against the broad-band continuum, enabling both efficient target selection with NB and MB filters and efficient redshift identification. We will select LAE using a traditional approach from MB imaging data based on identifying sources which show a photometric excess in the MB (see Fig. 9-Right). In practice, LAE candidates are selected using the magnitude difference between one of the two MB filters (MB1 or MB2) and Rubin/LSST broad-band (g or r). This methodology has been successfully tested using DESI spectroscopic follow-up of LAE candidates selected from IBIS imaging. Figure 9-Left shows five examples, for LAE candidates selected using the five MB filters of IBIS. With several DESI-II pilot programs, DESI successfully measured redshifts for the $2.3 < z < 3.4$ redshift range with Ly- α line fluxes $F(\text{Ly}\alpha) \geq 1 \times 10^{-16} \text{ erg s}^{-1} \text{ cm}^{-2}$ with a 70–80% success rate. In the case of POLU, with the two bluest MB filters, we will cover the $2.3 < z < 2.7$ redshift range.

For selecting LBGs, we will use a standard ‘dropout technique’, as shown on Fig. 10-Right, which identifies UV-bright high-redshift galaxies based on a continuum break at the Lyman limit and / or at the Ly α line due to absorption by neutral hydrogen (see Fig. 10). This method has been extensively tested using broad-band imaging, for instance, with CLAUDS imaging (Sawicki et al. 2019) in DESI pilot surveys (Ruhmann-Kleider et al. 2024). What we propose here is a method that builds on this approach. By combining the two MB1 and MB2 medium-band filters, we can use the resulting 520Å-wide composite-band with Rubin/LSST g, r bands to select sources which ‘drop out’ in the composite band; these are LBG candidates at $2.7 < z < 3.4$.

The POLU survey provides an optimal imaging for both LAE and LBG selections, which are complementary in redshift. The current strategy is to divide the five MB filter imaging between the POLU survey at CFHT and the IBIS survey at CTIO, using the two bluest MB for POLU given the sensitivity of MegaCam in the blue. We already have all five filters for DECam and have taken pilot observations in the IBIS survey, which has allowed us to test this target selection of LAEs and LBGs, using the five bands with a follow-up on DESI in COSMOS and XMM fields. We have demonstrated that we can achieve densities of 1,000 to 2,000 targets per square degree and achieve a probability of determining a secure redshift greater than 70% with exposure times of one to two hours.

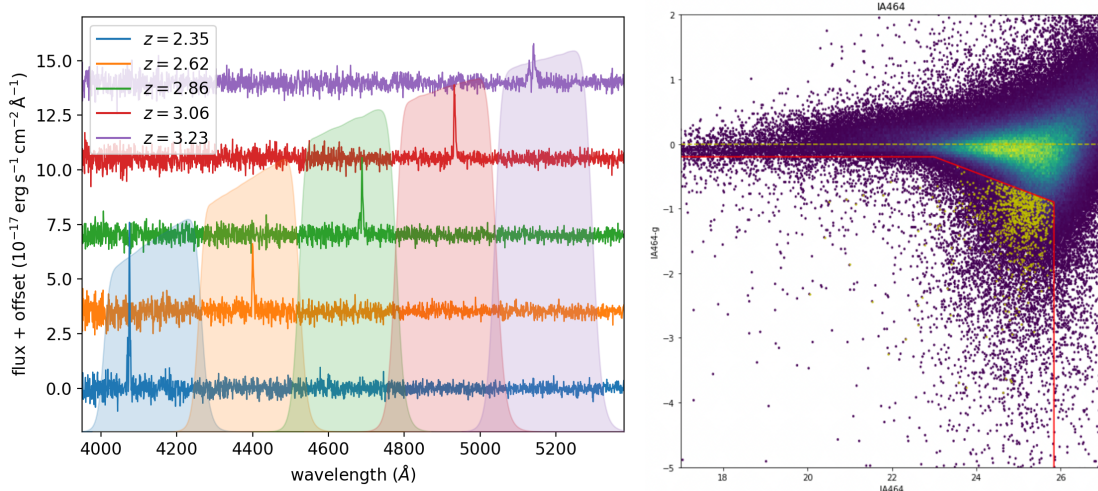


Figure 9. Left: Example spectra of LAEs observed in a DESI-II pilot program. They were selected using IBIS imaging. The fluxes are offset for better visibility. Each spectrum has 1 hour of effective exposure time. **Right:** LAE selection with Subaru/SuprimeCam MB filter, IA464: the red line shows the LAE selection box.

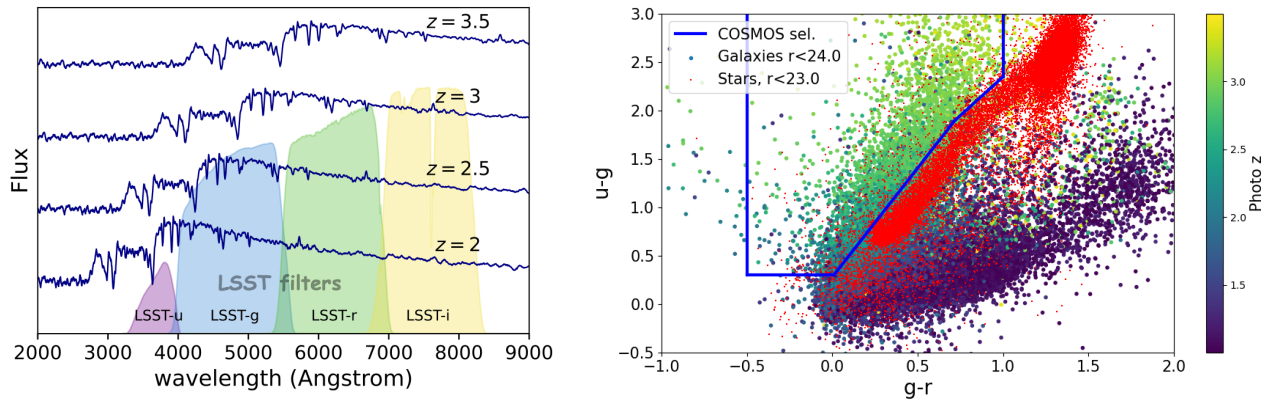


Figure 10. Left: Effective DESI LBG spectrum spanning the redshift range $2 \leq z \leq 4$ (by stacking individual LBG spectra observed with DESI (Ruhmann-Kleider et al. 2024)). **Right:** u -dropout selection of LBGs with CLAUDS: the blue line shows the LBG selection box, red dots are HSC stars and medium size dots coloured by photometric redshift, LEPHARE (Arnouts et al. 1999, Arnouts et al. 2002) are HSC galaxies.

1.2.2 SD2.2: Integration times

We have carried out a detailed study to estimate the observation time required to detect at 5σ the Ly- α line of a LAE. Using a Ly- α luminosity function from the literature, we select line fluxes to achieve the same number of LAE galaxies in the two filters. The calculations are summarised in Table 1. We find that we need respectively for the MB1 4000 – 4260Å and the MB2 4260 – 4520Å filters, a total of 936 s and 884 s in dark conditions and delivered image quality of 0.8 arcsec. This includes MegaCam readout time for four sub-exposures. We have assumed PSF model photometry. We plan to use the dynamic observing time mode (QSO-SNR) in order to produce a survey of the best uniformity possible. We aim to observe the 4200 deg² footprint with four large dithers (a significant fraction of the MegaCam field of view). Assuming an average of 5.0 hours per night, this represents **a total of 430 nights for the whole POLU survey**. The number of nights required to reach a depth of magnitude 25.0, as determined by a simulation, will be validated by the first observations in the summer of 2026 using the final filters. We will then adjust the depth target to ensure a consistent depth across the entire survey within a budget of 430 nights. The sister program to this proposal on the Blanco telescope (IBIS; NOIRLab Proposal ID # 2023B-184194; ID # 2023B-184194; Schlegel and Dey, co-PIs) IBIS is using three redder MBs than the ones proposed here, and the CFHT time with MegaCam’s excellent blue sensitivity is critical to the overall program. IBIS has already been assigned 90 nights during the 2023B-2026A semesters followed by 263 nights awarded in a second proposal. We aim to complete the POLU observations on a similar timescale, starting in 2027. It is important to have at least 1000 deg² complete by the start-up of DESI-II in 2029, i.e. at least 100 nights for POLU before 2029.

Filter Wavelength	MB1 4000 – 4260Å	MB2 4260 – 4520Å
Ly- α flux [10^{-16} erg s $^{-1}$ cm $^{-2}$]	1.66	1.43
Source brightness [mag.]	25.00	25.00
Sky brightness [mag/arcsec 2]	22.27	22.28
Exposure time per dither [s]	194	181
Total time per tile [s]	936	884
Total exposure time for 4200 deg 2 [hours]	1092	1031
Total exposure time for 4200 deg 2 [nights]	218	206

Table 1. Exposure times required to detect a Ly- α line at a given line strength at 5σ . The total exposure time is computed for 4 exposures with a 40-second overhead and a 4200 deg 2 footprint.

1 .2.3 SD2.3: Footprint and observation strategy

POLU survey, which will observe an equatorial field, will be associated with the MB surveys, IBIS, at CTIO with DECam, Niji at Subaru Telescope with HSC and broad-band imaging such as the Rubin/LSST and Euclid surveys. The POLU and IBIS surveys will share the same coverage, but the former will observe the two bluest bands, while the latter will observe the three reddest MB. Niji, on the other hand, will be completely independent and will observe in the four bluest MBs. The filters for the five bands have been defined in exactly the same way so that the three surveys can be combined into a single survey in the end. The final surface area of the combination of the three surveys will be approximately 5,000 deg 2 , with 4,200 deg 2 allocated to POLU+IBIS and 800 square degrees to Niji. The 4200 deg 2 POLU footprint (see Fig. 3) is divided into two equatorial fields: a 1600 deg 2 rectangular strip in the South Galactic Cap and the union of two rectangular strips in the North Galactic Cap covering 2600 deg 2 . POLU will therefore request observing nights split between the A and B semesters with a good balance between the two semesters. The MB filters for POLU are manufactured by Asahi, which produced the same filters with the same specifications for the two associated surveys, IBIS and Niji, making the inter-calibration more robust. Their delivery is expected in May 2026. Tests with these new filters at CFHT will probably take place during the engineering time in June. We have planned five deep fields (including the COSMOS and XMM fields) for the overall survey (POLU+IBIS), which can be observed alternately throughout the year. We will use one of these five deep fields to validate the new filters at the CFHT.

2. Minimum number of nights and survey strategy

This project has been designed for a timely and competitive CS aimed at providing a unique set of data not accessible at any other ground-based or space facility, to address several open questions in astrophysics and cosmology. It is thus of interest for a very wide community, spanning from local studies of star formation and ISM in the MW, to LG, large scale structures, the high- z Universe, and cosmology. The number of requested nights has been designed for this purpose; thus, any significant cut (>10 – 20%) would automatically result in the exclusion of a community to the dataset, hampering the CS nature of this proposal. Moreover our request of 700 nights is also motivated by the challenging nature of these large time allocations which might reach completion rates of the order of 80–100%. With the weather being the most significant risk of the project we envision a shared risk between the two sub-surveys which will equally share the weather conditions, and a yearly monitoring of the sub-surveys data quality and progress, to evaluate corrections to the survey strategy.

3. Data and Project Management Plan

WP-D.1: Data Reduction and Analysis. Different pipelines optimised for the detection of point (POLU) and extended (StarFEAST) sources will be used for the two sub-surveys, as described below:

StarFEAST (*Lead: J.C. Cuillandre, M. Fossati, E. Mangola*)

The StarFEAST project will benefit from the end-to-end pipeline developed to support the VESTIGE survey. The Elixir data distributed by CFHT will be run through Elixir-LSB – a pipeline developed within the NGVS collaboration (Ferrarese et al. 2012) to detect extended LSB features, and later applied successfully to the VESTIGE survey. The Elixir-LSB pipeline has been automated at CADC for CFIS activities. Global astrometric solutions, image stacking and source catalogues will then be generated at CADC by MegaPipe. Members of our team have developed extensive software for the detection and the analysis of extended and point sources in broad-band and NB images (Cuillandre, Stone). The reduced data will be combined with those at other frequencies to produce a complete, unique dataset for the observed regions.

POLU (*Lead: D. Lang, A. Raichoor*)

The aim is to combine the POLU observations with other MB observations and broad-band observations. The team’s philosophy is to make the catalogs available to the astrophysical community as quickly as possible, adopting a similar structure to that used for DECaLS (<https://www.legacysurvey.org/decamls/>). The data reduction plan splits into two efforts. We plan to run image-level reductions and calibrations at CADC-CANFAR, and then copy calibrated image products to the US National Energy Research Scientific Computing center (NERSC) for catalog-level reductions. Calibrated, coadded images will be provided with the catalog releases (the *Tractor*-based reductions are performed on individual images rather than coadds, but coadds remain a useful data product for other science cases and other users of the data). Our team has successfully obtained sufficient storage and computing resources at NERSC for the computationally-intensive reductions we have planned, using the *Legacypipe/Tractor* pipeline. These resources are allocated through the US Department of Energy’s High Energy Physics program allocation, and has included approximately 50 million CPU-hours for each of the DESI Legacy Imaging Surveys Data Releases 9 and 10. We expect to successfully compete for sufficient compute resources for the reduction and release of this MB imaging campaign (including POLU and the DECam MB imaging survey), along with the corresponding broad-band imaging.

WP-D.2: Data Distribution and Publication Plan. (*Lead: A. Boselli, C. Yèche, D. Lang, Y. Roehly, A. Raichoor*)

Our proposed community survey will be public with no proprietary period. Both for StarFEAST and POLU, the raw data will be available immediately, with image-level reductions available shortly after each observing run at CADC-CANFAR. Catalog-level data releases will occur yearly, with a first early data release within one year of the first semester of observation. Each data release will reprocess all previous data from this program to take advantage of pipeline improvements and provide uniformity of the data within each release. A final data release with all data will be completed no more than 1 year after the completion of observing. For StarFEAST, the data will be released through a CeSAM (LAM Marseille) dedicated web-interface, as successfully done for several previous projects lead by our team (HRS <http://hedam.lam.fr/HRS/>; GUViCS <https://observations.lam.fr/guvics/>; VESTIGE <https://mission.lam.fr/vestige/>). High level science products and catalogs obtained by ad-hoc analysis for specific science goals will be released after the last data release. For POLU, catalog-level products and calibrated images will be made available through NERSC and through the NOIRLab Science Archive. NERSC access methods include simple https, Globus Online for bulk data transfer, and custom web applications based on the Spin service (<https://www.nersc.gov/systems/spin/>). In addition, we will provide public access to catalogs through the NOIRLab Astro Data Lab service. Finally, all released data will be copied to the NERSC HPSS Archive system (<https://www.nersc.gov/systems/hpss-data-archive/>) for safe, long-term storage. The imaging data will also be served through the interactive sky viewer (<https://www.legacysurvey.org/viewer/>) custom built by co-PI Lang for the Legacy Surveys project. This also provides a compelling public engagement platform, where members of the public can explore the beautiful images collected by these surveys. Our teams are very experienced in the execution of large imaging surveys, pipeline reduction, and the reduction and public release of calibrated, useful, and well-documented survey data products in a timely way (see for instance, DECaLS: <https://www.legacysurvey.org/decamls/>).

The results of StarFEAST and POLU will be published in refereed journals with an high overall publication rate significantly (~50 refereed publications within three years of the completion of the survey) given the large involvement of scientists of different communities. Finally, in addition to the large number of CFHT citations and acknowledgements that can be expected from the DESI-2 project and the scientific papers using StarFEAST and POLU data, the public catalogs and images will give even greater benefit to the CFHT.

WP-D.3: Outreach. (*Lead: S. Boissier, J.C. Cuillandre, P. Zarrouk*)

This CS will provide a large number of spectacular images of star forming regions within the MW, of LG, and of interacting systems in large scale structures. These images are perfectly suited for CFHT outreach communications, for the well known CFHT calendar, for planetarium activities, and for dedicated press releases. The entire POLU team will reuse all the infrastructure developed for DECaLS, particularly the sky viewer, <https://www.legacysurvey.org/viewer/>, which provides a sky map that offers tremendous benefits for all outreach activities.

WP-D.4: Support Offered to the QSO Team. (*Lead: J.C. Cuillandre, B. Epinat*)

The StarFEAST team, with two decades of expertise on MegaCam and CFHT observing, can contribute to data processing, starting from raw data if the operation of the Elixir pipeline at CFHT represents an obstacle. We can implement tools to monitor the survey’s status on a run-to-run basis and incoming data, aiding the validation process. We commit to regularly updating the status of the CS, clearly indicating priorities for each run to assist the QSO team’s decision-making process.

The POLU team has a strong history of working closely with the DECam/Blanco staff to carry out the DECaLS and IBIS surveys in a way that uses telescope time very efficiently and requires little support from the observatory staff. We

have produced real-time monitoring systems to track and adapt to the sky conditions, adjusting exposure times to reach our target depths. This allows us to observe faster in good sky conditions, and also still make good use of less than perfect conditions, in a fully automated fashion. We provide observers for all observing runs, and have made our tools available to other facility users.

WP-D.5: Follow-up observations. (*Lead: D. Lang, F. de Gasperin, P. Serra, M. Sun*)

Multifrequency follow-up observations might be necessary for the best scientific exploitation of the data. Spectroscopic observations, required for the redshift measurement of unclassified local and high- z line emitters, or to supplement the properties of the detected sources ([NII] contamination, dust attenuation, line diagnostic diagrams) will be taken from public archives or from dedicated follow-up campaigns using MOS facilities such as DESI, WEAVE or Subaru PFS. Thanks to the large involvement of the community to this project, we will have access to several ground-based or space-based facilities such as ASKAP, LOFAR, MeerKAT, VLT, DESI, WEAVE, Dragonfly, PRIMA, UVIT, CASTOR, XMM, NewATHENA, granting the access to all the data necessary for the best scientific exploitation of the CFHT data.

4. Team Expertise.

StarFEAST: The team has more than 20 years of expertise in the acquisition, data reduction, and scientific exploitation of MegaCam data. It includes PIs of several successful CFHT LPs (NGVS, Ferrarese; CFIS, Cuillandre; VESTIGE, Boselli). Several team members are deeply involved in the different synergic surveys, other have extensive experience in the acquisition, reduction and analysis of NB imaging (Boselli et al. 2018, Lokhorst et al. 2022). They also have experience in the reduction of radio continuum and HI (de Gasperin et al. 2025; Serra et al. 2023), CO (Braine et al. 2010; Jachym et al. 2014; Brown et al. 2021) and X-rays (Sun et al. 2007) data to which $H\alpha$ data will be confronted. Others have developed SED fitting codes (CIGALE, Boquien et al. 2019) or have a unique expertise in 2D chemo-spectrophotometric and dynamical models of galaxy evolution (Boissier & Prantzos 1999) and in hydrodynamic simulations of gas stripping in dense environments (Vollmer et al. 2021; Renaud et al. 2014; Boselli et al. 2021; Woods et al. 2024) including cosmological simulations (Ahvazi et al. 2024; Kraljic et al. 2020) – all powerful tools for the analysis and interpretation of the NB imaging data. Overall, the team includes recognized leaders in the study of star forming regions in the MW (Russeil 2003; Zavagno et al. 2006), LG (Boquien et al. 2015; Melchior et al. 2016; Braine et al. 2018; Lokhorst et al. 2022), the effects of the environment on galaxy evolution (Vollmer et al. 2001; Yagi et al. 2010; Kenney et al. 2015; Boselli et al. 2022), LFs (Ferrarese et al. 2016; Cuillandre et al. 2025), LSB systems (Boissier et al. 2016; Lokhorst et al. 2022), star formation (Boselli et al. 2009; Braine et al. 2010; Boquien et al. 2019; Woods et al. 2024), dwarf (Côté et al. 2009; Taylor et al. 2018) and high- z galaxies (Fossati et al. 2017), including line-emitting systems (Epinat et al. 2012, 2024; Fossati et al. 2017), and the dynamical evolution of clusters (Kraljic et al. 2018). We therefore have the access, resources, and expertise to fully capitalize on this unique dataset which will also be used to train students, postdocs, and highly qualified personnel.

POLU: One of the strengths of the POLU team is that it combines the French and Canadian teams for the science with an international team, DECaLS, with extensive expertise in data processing. This team has consistently delivered source catalogs for DESI target selection on time, including DR9 for DESI (Dey et al. 2019) and DR11 for the DESI extension. The team has also demonstrated its ability to coordinate observations and data reduction for the benefit of other projects (for instance, 4MOST with the DR9 release and eROSITA with the DR10 release). In the field of science, all members of DESI and later DESI-II are recognized as global leaders in the processing of 3D catalogs with redshifts and clustering science in general. The number of publications and citations of their main papers (Adame et al. 2025, Abdul-Karim et al. 2025), which exceeds 2,500, is a clear indicator of this. In addition to their extensive expertise in 3D catalogs, the entire team has extensive experience in the scientific analysis of imaging catalogs, whether it involves photometric redshift determination (Arnouts et al. 1999, Arnouts et al. 2002, Ilbert et al. 2006), studies of dark matter in dwarf galaxies (Leauthaud et al. 2020, Luo et al. 2024), directly the measurement of 2D clustering (Payerne et al. 2025, Ebina et al. 2026) or study of cross correlation with (CMB lensing or kSZ) (Zhou et al. 2023, Krolewski et al. 2024, Chaussidon et al. 2026). For over a decade, the team has worked with DESI to conduct pilot surveys, acquiring significant expertise in identifying star-forming galaxies, including LBGs (Ruhlmann-Kleider et al. 2024, Payerne et al. 2025) and LAEs (Ebina et al. 2024). In addition, the project will enable unprecedented studies of galactic building blocks and cosmic web structures across cosmic time (Bacon et al. 2021), while the team’s strong expertise in this field ensures they are well equipped to fully exploit these advanced observations with BlueMUSE (Richard et al. 2019). In conclusion, POLU’s PI team brings well-established expertise in image processing, along with a deep understanding of the scientific knowledge that can be extracted from it. This strength is further enhanced by the DESI environment, which offers access to a broad and highly qualified talent pool.

References

Abdul-Karim et al. 2025, Phys. Rev. D, 112, 083515; Adame et al. 2025, JCAP, 028; Adams et al. 2022, A&A, 667, 38; Ahvazi et al. 2024, OJAp, 7, 111; Arnouts et al. 1999, MNRAS, 310, 540; Arnouts et al. 2002, MNRAS, 329, 355; Bacon et al. 2021, A&A, 647, A107; Baldwin et al. 1981, PASP, 93, 5; Boissier & Prantzos 1999, MNRAS 307 857; Boissier et al. 2016, A&A, 593, 126; Boquien et al. 2015, A&A, 578, 8; Boquien et al. 2019, A&A, 622, 103; Boselli & Gavazzi 2006 PASP 118 517; Boselli et al. 2009, ApJ, 706, 1527; Boselli et al. 2016, A&A, 587, 68; Boselli et al. 2018, A&A, 614, 56; Boselli et al. 2019, A&A, 631, 114; Boselli et al. 2021, A&A, 646, 139; Boselli et al. 2022, A&A Rev, 30, 3; Boselli et al. 2026, A&A, submitted; Braine et al. 2010, A&A, 518, L69; Braine et al. 2018, A&A, 612, 51; Brown et al. 2021, ApJS, 257, 21; Chaussidon et al. 2026, arXiv:2604.04867; Côté et al. 2009, AJ, 138 1037; Cote et al. 2025, JATIS, 11, 2202; Cowie & Songaila 1977, Nat 266, 501; Cowie et al. 1996, AJ, 112, 839; Cuillandre et al. 2025, A&A, 697, 11; Dave et al. 2019, MNRAS, 486, 2827; De Gasperin et al. 2021, A&A, 648, 104; Dey et al. 2019, AJ, 157, 168; Dressler et al. 1997, ApJ, 490, 577; Dressler et al. 2004, Carnegie conf 206; Drew et al. 2005, MNRAS, 362, 753; Drew et al. 2014, MNRAS, 440, 2036; Dubois et al. 2021, A&A, 651, 109; Eales et al. 2010, PASP, 122, 499; Ebina et al. 2024, JCAP, 052; Ebina et al. 2026, JCAP, 019; Emig et al. 2025, ApJ, 992, 216; Emsellem et al. 2022, A&A, 659, 191; Epinat et al. 2012, A&A, 539, 92; Epinat et al. 2024, A&A, 683, 205; Erb et al. 2011, ApJ, 740, 31; Ferrarese et al. 2012, ApJS, 200, 4; Ferrarese et al. 2016, ApJ, 824, 10; Fossati et al. 2017, ApJ, 835, 153; Galitzki et al. 2018, arXiv:1810.02465; Gavazzi et al. 2013, A&A, 553, 90; Geller & Huchra 1989, Sci 246, 897; Gwyn et al. 2025, AJ, 170, 324; Ilbert et al. 2006, A&A, 457, 841; Jachym et al. 2014, ApJ, 792, 11; Jarrett et al. 2019, ApJS, 245, 25; Huchra et al. 2012, ApJS, 199, 26; Kenney et al. 2015, AJ, 150, 59; Kennicutt 1998, ARA&A, 36, 189; Kraljic et al. 2018, MNRAS, 474 547; Kraljic et al. 2022, MNRAS, 514, 1359; Krolewski et al. 2024, JCAP, 021; Intema et al. 2017, A&A, 598, A78; Lada 1985, ARA&A, 23, 267; Larson et al. 1980, ApJ, 237, 692; Leauthaud et al. 2020, PDU, 30, 100719; Lee et al. 2024 ApJ, 962, 36; Lokhorst et al. 2022, ApJ, 927, 136; Luo et al. 2024, MNRAS, 530, 4988; Massey et al. 2006, AJ, 131, 2478; Melchior et al. 2016, A&A, 585, 44; Mentuch Cooper et al. 2023, ApJ, 943, 177; Merritt 1983, ApJ, 264, 24; Molinari et al. 2010, A&A, 518, L100; Mondelin et al. 2026, submitted; Moore et al. 1998, ApJ, 495, 139; Ouchi et al. 2008, ApJS, 176, 301; Payerne et al. 2025, JCAP, 031; Payerne et al. 2025, arXiv:2511.22243; Peng et al. 2010, ApJ, 721, 193; Pullen et al. 2015, MNRAS, 449, 4326; Ramakrishnan et al. 2023, ApJ, 951, 119; Reddy et al. 2009, ApJ, 692, 778; Reddy et al. 2022, ApJ, 926, 31; Renaud et al. 2014, MNRAS 442, 33; Richard, 2019, arXiv:1906.01657; Rousseau-Nepton et al. 2019, MNRAS, 489, 5530; Ruhlmann-Kleider et al. 2024, JCAP, 059; Russeil 2003, A&A, 397, 133; Sawicki et al. 2019, MNRAS, 489, 5202; Schaye et al. 2015, MNRAS, 446, 521; Serra et al. 2023, A&A, 673, 146; Shimwell et al. 2017, A&A, 598, A104; Slosar et al. 2008, JCAP, 031; Springel et al. 2018, MNRAS, 475, 676; Steidel et al. 2000, ApJ, 532, 170; Sun et al. 2007, ApJ, 671, 190; Sun et al. 2026, A&A, 705, 139; Taylor et al. ApJ, 2018, 867, L15; Tessyer et al. 2002, A&A, 385, 337; Tonnesen & Bryan 2010 ApJ, 709, 1203; Tornotti et al. 2025, A&A, 704, 201; Vollmer et al 2001, ApJ, 561, 708; Vollmer et al 2021, A&A 645, 121; Watkins et al. 2023, ApJL, 944, L24; Wilman et al. 2010, MNRAS, 406 1701; Woods et al. 2024, ApJ, 960, 59; Xie et al. 2025, A&A, 698, 73; Yagi et al. 2010, AJ, 140, 1814; Yu et al. 2022, MNRAS 513, 1887; Zavagno et al. 2006, A&A, 446, 161; Zhang et al. 2021, ApJ, 922, 167; Zhou, et al. 2023, JCAP, 097;

Co-investigators for StarFEAST

Name	Email	Name	Email
Philippe Amram	philippe.amram@lam.fr	Paola Andreani	pandrea@eso.org
Emmanuel Bertin	bertin@iap.fr	Samuel Boissier	samuel.boissier@lam.fr
Micol Bolzanella	micol.bolzanella@inaf.it	Sylvain Bontemps	sylvain.bontemps@u-bordeaux.fr
Mederic Boquien	mederic.boquien@oca.eu	Jonathan Braine	jonathan.braine@u-bordeaux.fr
Thobias Brown	Tobias.Brown@nrc-cnrc.gc.ca	Veronique Buat	veronique.buat@lam.fr
Denis Burgarella	denis.burgarella@lam.fr	Francesco Calura	francesco.calura@inaf.it
Barbara Catinella	barbara.catinella@uwa.edu.au	Laurent Chemin	laurent.chemin@astro.unistra.fr
Thierry Contini	Thierry.Contini@omp.eu	Luca Cortese	luca.cortese@uwa.edu.au
Patrick Cote	Patrick.Cote@nrc-cnrc.gc.ca	Timea Csengeri	timea.csengeri@u-bordeaux.fr
Jean-Charles Cuillandre	jcc@cfht.hawaii.edu, jc.cuillandre@cea.fr	Anne Decourchelle	anne.DECOURCHELLE@cea.fr
Francesco deGasperin	francesco.degasperin@inaf.it	Gabriella De Lucia	gabriella.delucia@inaf.it
Laurent Drissen	Laurent.Drissen@phy.ulaval.ca	Sara Ellison	sarae@uvic.ca
Benoit Epinat	benoit.epinat@lam.fr	Laura Ferrarese	lauraFerrarese1@gmail.com
Matteo Fossati	matteo.fossati@unimib.it	Michele Fumagalli	michele.fumagalli@unimib.it
Marie-Lou Gendron-Marsolais	marie-lou.gendron-marsolais@phy.ulaval.ca	Emilie Habart	emilie.habart@ias.u-psud.fr
Gerhard Hensler	gerhard.hensler@univie.ac.at	Pavel Jachym	jachym@ig.cas.cz
Jeff Kenney	jeff.kenney@yale.edu	Katarina Kraljic	kraljic@unistra.fr
Dustin Lang	dstndstn@gmail.com	Francois Levrier	francois.levrier@ens.psi.eu
Deborah Lokhorst	Deborah.Lokhorst@nrc-cnrc.gc.ca	Alessandro Loni	alessandro.loni@inaf.it
Alessandro Lupi	alessandro.lupi@uninsubria.it	Gary Mamon	gam@iap.fr
Elena Mangola	elena.mangola@lam.fr	Silvia Martocchia	silvia.martocchia@lam.fr
Sophie Maurogordato	sophie.maugordato@oca.fr	Alan McConnachie	alan.mconnachie@nrc-cnrc.gc.ca
Anne-Laure Melchior	Anne-Laure.Melchior@obspm.fr	Marc-Antoine Miville-Deschenes	marc-antoine.miville-deschenes@cna.fr
Maelie Mondelin	maelie.mondelin@cea.fr	Cameron Morgan	crmorgan@uwaterloo.ca
Frederique Motte	frederique.motte@univ-grenoble-alpes.fr	Julio Navarro	jfn@uvic.ca
Thomas Nony	thomas.nony@u-bordeaux.fr	Parisa Nozari	21pn10@qweensu.ca
David Patton	dpatton@trentu.ca	Roser Pello	rosier.pello@lam.fr
Jerome Pety	pety@iram.fr	Florent Renaud	florent.renaud@astro.unistra.fr
Yannick Roehly	yannick.roehly@lam.fr	Carmelle Robert	Carmelle.Robert@phy.ulaval.ca
Joel Roediger	joel.roediger@nrc-cnrc.gc.ca	Delphine Russeil	delphine.russeil@lam.fr
Sarah Sadavoy	sarah.sadavoy@qweensu.ca	Marc Sauvage	marc.sauvage@cea.fr
Carlo Schimd	carlo.schimd@lam.fr	Nicola Schneider	nschneid@ph1.uni-koeln.de
Paolo Serra	paolo.serra@inaf.it	Connor Stone	connorstone628@gmail.com
Ming Sun	ms0071@uah.edu	Matthew Taylor	matthew.taylor2@ucalgary.ca
Davide Tornotti	davide.tornotti@unimib.it	Bernd Vollmer	bernd.vollmer@astro.unistra.fr
Tyron Woods	Tyrone.Woods@umanitoba.ca	Christophe Yèche	christophe.yeche@cea.fr
Masafumi Yagi	YAGI.Masafumi@nao.ac.jp	Annie Zavagno	annie.zavagno@lam.fr

The MegaCam CFHT CS – StarFEAST and POLU

Co-investigators for POLU, Canada and Hawaii

Name	Institution	Name	Institution
Alan McConnachie	NRC Herzberg Astronomy & Astrophysics	Julio Navarro	University of Victoria
Kim Venn	University of Victoria	Scott Wilkinson	University of Victoria
Allison Man	University of British Columbia	Meng-Xiang Lin	Simon Fraser University
Joanna Woo	Simon Fraser University	Denis Leahy	University of Calgary
Nassim Bozorgnia	University of Alberta	Stanimir Metchev	Western University
Mike Hudson	University of Waterloo	Will Percival	University of Waterloo
James E. Taylor	University of Waterloo	Caio B. de S. Nascimento	Perimeter Institute for Theoretical Physics
Neal Dalal	Perimeter Institute for Theoretical Physics	Katie Mack	Perimeter Institute for Theoretical Physics
Kendrick Smith	Perimeter Institute for Theoretical Physics	Suroor Seher Gandhi	Perimeter Institute for Theoretical Physics
Pat Hall	York University	Ting Li	University of Toronto
Jo Bovy	University of Toronto	Josh Speagle	University of Toronto
Nathan Sandford	University of Toronto	David Patton	Trent University
Patrick Dufour	Université de Montréal	John Ruan	Bishop's University
Weixiang Yu	Bishop's University	Ivana Damjanov	Saint Mary's University
Vincent Hénault-Brunet	Saint Mary's University	Kenneth Chambers	University of Hawaii

Co-investigators for POLU, France

Name	Institution	Name	Institution
Eric Armengaud	Irfu, CEA, Université Paris-Saclay	Etienne Burtin	Irfu, CEA, Université Paris-Saclay
Arnaud De-Mattia	Irfu, CEA, Université Paris-Saclay	Constantin Payerne	Irfu, CEA, Université Paris-Saclay
Jean-Charles Cuillandre	Irfu, CEA, Université Paris-Saclay	Nathalie Palanque-Delabrouille	Irfu, CEA, Université Paris-Saclay
Edmond Chaussidon	Irfu, CEA, Université Paris-Saclay	Johan Richard	Centre de Recherche Astrophysique de Lyon
Anand Raichoor	APC, Université Paris Cité	Stéphane Arnouts	Laboratoire d'Astrophysique de Marseille
Alessandro Boselli	Laboratoire d'Astrophysique de Marseille	Eric Jullo	Laboratoire d'Astrophysique de Marseille
Raphael Gavazzi	Laboratoire d'Astrophysique de Marseille	Olivier Ilbert	Laboratoire d'Astrophysique de Marseille
Matthew Pieri	Laboratoire d'Astrophysique de Marseille	Laurence Tresse	Laboratoire d'Astrophysique de Marseille
Sylvain De La Torre	Laboratoire d'Astrophysique de Marseille	Nicolas Martin	Observatoire Astronomique de Strasbourg
Katarina Kraljic	Observatoire Astronomique de Strasbourg	Clothilde Laigle	Institut d'Astrophysique de Paris
Patrick Petitjean	Institut d'Astrophysique de Paris	Pauline Zarrouk	LPNHE, Sorbonne Université
Laurent Le Guillou	LPNHE, Sorbonne Université	Théo Simon	LPNHE, Sorbonne Université
Agnès Ferté	LPNHE, Sorbonne Université	Corentin Ravoux	LPCA Clermont
Stéphanie Escoffier	CPPM, Marseille	Julian Bautista	CPPM, Marseille
Alice Pisani	CPPM, Marseille	William Gillard	CPPM, Marseille
Pauline Vielzeuf	CPPM, Marseille		